

# Massive Binary Black Holes in the Cosmic Landscape

Monica Colpi<sup>1</sup> & Massimo Dotti<sup>2</sup>

1-Department of Physics G. Occhialini, University of Milano-Bicocca,  
Piazza della Scienza 3, 20126 Milano, Italy, colpi@mib.infn.it

2-Department of Astronomy, University of Michigan,  
Ann Arbor, MI, 48109, USA, mdotti@umich.edu

## Abstract

*Binary* black holes occupy a special place in our quest for understanding the evolution of galaxies along cosmic history. If massive black holes grow at the center of (pre-)galactic structures that experience a sequence of merger episodes, then dual black holes form as inescapable outcome of galaxy assembly, and can in principle be detected as powerful dual quasars. But, if the black holes reach *coalescence*, during their inspiral inside the galaxy remnant, then they become the loudest sources of gravitational waves ever in the universe. The *Laser Interferometer Space Antenna* is being developed to reveal these waves that carry information on the mass and spin of these binary black holes out to very large look-back times. Nature seems to provide a pathway for the formation of these exotic binaries, and a number of key questions need to be addressed: How do massive black holes pair in a merger? Depending on the properties of the underlying galaxies, do black holes always form a close Keplerian binary? If a binary forms, does hardening proceed down to the domain controlled by gravitational wave back reaction? What is the role played by gas and/or stars in braking the black holes, and on which timescale does coalescence occur? Can the black holes accrete on flight and shine during their pathway to coalescence? After outlining key observational facts on dual/binary black holes, we review the progress made in tracing their dynamics in the habitat of a gas-rich merger down to the smallest scales ever probed with the help of powerful numerical simulations. N-Body/hydrodynamical codes have proven to be vital tools for studying their evolution, and progress in this field is expected to grow rapidly in the effort to describe, in full realism, the physics of stars and gas around the black holes, starting from the cosmological large scale of a merger. If detected in the new window provided by the upcoming gravitational wave experiments, binary black holes will provide a deep view into the process of hierarchical clustering which is at the heart of the current paradigm of galaxy formation. They will also be exquisite probes for testing General Relativity, as the theory of gravity. The waveforms emitted during the inspiral, coalescence and ring-down phase carry in their shape the sign of a dynamically evolving space-time and the proof of the existence of an horizon.

Keywords: black hole physics - stellar and fluid dynamics - galaxies: evolution - galaxies: nuclei - galaxies: cosmology

## 1 Black holes in the cosmic landscape

### 1.1 Introduction

Massive black holes weighing from a million to a billion suns have long been suspected to be the powerhouse of energetic phenomena taking place in distant galaxies. Energy in the form of radiation, high velocity plasma outflows, and ultra relativistic jets, is extracted efficiently from the gravitational field of the black

hole when gas is accreting from the parsec scale of a galactic nucleus down to the scale of the horizon. Since the early discovery of quasars, the accretion paradigm has been at the heart of the interpretation of massive black holes as being "real" sources in the universe. It was also recognized in the late 60's that the luminous quasars and the active galactic nuclei (AGNs) were undergoing strong cosmic evolution: nuclear activity was common in the past and declined with cosmic time. No bright quasar lives in our local universe, but a few AGNs are present with very modest activity, representing the fading tail of the population. From simple considerations on the life-cycle of quasars, there has been always the suspicion that at high redshifts accretion was ignited in many if not all galaxies, leading to the commonly held premise that most galaxies we see in our local universe should host in their nucleus a massive black hole, relic of an earlier active phase.

For long times, black hole masses in AGNs and quasars have been inferred only indirectly using as chief argument the concept of Eddington limited accretion. But today, due largely to the impact of ground-based telescopes and of the Hubble Space Telescope, the mass of quiescent black holes inside the cores of nearby galaxies including our own Milky Way, has been measured using stars and/or gas clouds as dynamical probes. Now there is indeed strong circumstantial evidence that massive black holes are ubiquitous in ellipticals and in the bulges of disk galaxies. Astronomers discovered in addition, and most importantly, the existence of tight correlations between the black hole mass and the large scale properties of the underlying host<sup>1-7</sup>. It is currently believed that during the formation of galaxies, a universal mechanism was at play able to deposit, in the nuclear regions, large amounts of gas to fuel the black hole to such an extent that its feedback, i.e. its large-scale energy/momentum injection, had blown the gas out, thus sterilizing the galaxy against further star formation<sup>8-10</sup>. Major galaxy mergers could be at the heart of this symbiotic relationship as they may explain both the ignition of a powerful AGN and the formation of a violently perturbed galaxy remnant dominated by stellar dispersion<sup>11</sup>.

Galaxy formation is a genuine cosmological problem: the cooling and collapse of baryons in dark matter halos, clustering hierarchically, is the prime element for understanding galaxy evolution. The time of first appearance of black holes in mini-halos is largely unknown: whether they formed at redshift  $z \sim 20$  as relic of the first metal free stars<sup>12</sup>, or later in more massive virialized haloes from unstable gaseous disks or dense young star clusters, is unknown<sup>12-20</sup>. What is currently known is that black holes mainly grow from gas accretion<sup>21,22</sup>, and that bright quasars, hosting a billion solar mass black hole, are already in place out to redshift  $z \sim 6$  when the universe was  $\lesssim 10^9$  years old<sup>23</sup>. The new paradigm of the concordant evolution of black holes and galaxies imposes a new perspective: black holes previously believed to play a passive role are now in "action" shaping their cosmic environment<sup>24-25</sup>.

The coevolution of black hole and galaxies embraces a variety of astrophysical phenomena that are now becoming of major scientific interest. They go from the formation of black hole seeds in the first pre-galactic structures clustering hierarchically at very high redshifts, to black hole growth and feedback in major gas-rich mergers. But not only. A new and critical aspect of this concordant evolution is the presence of *black hole pairs* in galaxies that form during the violence of a merger. *There is growing evidence that Nature provides through mergers the privileged habitat where massive binary black holes can form and evolve.* But why are *binary black holes* important? The answer is manifold and is the focus of this writing.

The review is organized as follows. In Section 1.2 we introduce key physical scales of black hole binaries on their path to coalescence under the emission of gravitational waves. In Section 1.3 we summarize current evidence of dual and binary black holes in the realm of observations. Section 1.4 reports on the quest for the presence of massive black hole binaries in bright elliptical galaxies. Section 2 describes the basic physics

of black hole inspiral both in gas-poor and gas-rich environments also with use of numerical simulations. Section 3 summarizes selected results attained over the last years in the study of black hole hardening in pure stellar/collisionless backgrounds. Section 4 shows key results on the formation of black hole pairs/binaries during gas-rich major as well as minor mergers, simulated with unprecedented accuracy starting from cosmologically motivated initial conditions. In Section 5 we address a number of issues related to the dynamics of binary black holes in massive gaseous disks: orbital decay, eccentricity evolution, accretion on flight and migration in a circum-binary disk. Section 6 explores the delicate and important issue on the electromagnetic counterparts of gravitational wave coalescence events. Section 7 contains our conclusions and future perspectives.

## 1.2 Gravitational waves from binary black holes

Einstein’s theory of space-time and gravity, General Relativity, predicts that motions of masses produce propagating waves that travel through space-time at the speed of light  $c$ . Two masses (of total mass  $M_{\text{BH,T}}$ ) in a binary emit gravitational waves that in the far field zone, i.e. much farther away from the source, perturb space-time with a dimensionless metric-strain amplitude  $h_{\text{GW}} \sim (M_{\text{BH,T}}V_{\text{cir}}^2)/D$ , where  $D$  is the distance and  $V_{\text{cir}}$  the orbital velocity (in geometric units). This indicates that the strongest sources of gravitational waves are the most massive bodies that move close to the speed of light, i.e. the most massive black holes ( $M_{\text{BH,T}} \sim 10^6 - 10^9 M_{\odot}$ ) that move in a binary, with  $V_{\text{cir}} \sim c$ , at the moment of their coalescence. Therefore, binary black holes ”created” in merging galaxies offer one of the most promising venues of producing the loudest gravitational waves in the universe that the *Laser Interferometer Space Antenna (LISA)* or/and the Pulsar Timing Array (PTA) experiment are expected to detect<sup>26–34</sup>. During late inspiral and final plung-in, the black holes become genuine dynamical entities, creating rich space-time structure that remains imprinted in the strain amplitude signal. The detection of this signal gives unique probe of the existence of the horizon which clothes the interior singularity of the black hole.

According to the *no-hair* theorem, a black hole is similar to an elementary particle specified uniquely by its mass  $M_{\text{BH}}$  and angular momentum  $\mathbf{J}_{\text{BH}}$  (dimensionless spin  $\hat{a} = cJ_{\text{BH}}/GM_{\text{BH}}^2 \leq 1$ ). The size of the horizon that varies from  $2GM_{\text{BH}}/c^2$  for  $\hat{a} = 0$  to  $GM_{\text{BH}}/c^2$  for  $\hat{a} = 1$  (for a maximally rotating Kerr hole) is very tiny compared to the galactic scale: for  $\hat{a} = 0$ , the horizon is  $3 \times 10^{11}(M_{\text{BH}}/10^6 M_{\odot})$  cm, i.e. only  $10^{-7}(M_{\text{BH}}/10^6 M_{\odot})$  pc (considering that one pc is the mean distance between the stars in the solar neighborhood). Thus only through the detection of the waveforms emitted from ”coalescing” and ”vibrating” black holes we may hope to unravel their true nature<sup>35</sup>. With *LISA*, black hole masses and spins will be measured with astonishing accuracy<sup>36,37</sup>, and this claim suffices to explain why binary black holes are becoming now so important not only for exploiting the black hole demography in a cosmological context, but gravity in the strong field regime. As two black holes of mass  $M_{\text{BH,1}}$  and  $M_{\text{BH,2}}$  coalesce, a new black hole forms with mass less than the sum  $M_{\text{BH,1}} + M_{\text{BH,2}}$  according to the area theorem. Gravitational waves carry away mass-energy and angular momentum, and depending on the spin, they carry away also linear momentum as the resulting radiation pattern is anisotropic. The binary center of mass thus recoils back and the relic black hole acquires a kick<sup>38–43</sup>. While for slowly spinning black holes and for spins (anti-)aligned with the orbital axis, recoil velocities are  $\lesssim 400 \text{ km s}^{-1}$ , there are spin configurations for which the recoil can be as large as  $4000 \text{ km s}^{-1}$ , i.e. in excess of the escape velocity from the largest galaxies: this occurs when the black holes have comparable masses, and the spin vectors have opposite directions and lie in the orbital plane.

*Coalescence* and *recoil* are the final step of a long process of *slow inspiral*. According to the quadrupole

formula, a binary of total mass  $M_{\text{BH,T}}$ , mass ratio  $q_{\text{BH}} = M_{\text{BH,2}}/M_{\text{BH,1}} \leq 1$ , semi-major axis  $a$ , and eccentricity  $e$ , is expected to coalesce, i.e. to reduce its axis  $a$  virtually to zero, after a time span<sup>44</sup>

$$t_{\text{GW}} = \frac{5}{256} \frac{c^5}{f(e) G^3} \frac{(1 + q_{\text{BH}})^2}{q_{\text{BH}}} \frac{a^4}{M_{\text{BH,T}}^3}, \quad (1)$$

where  $f(e) = [1 + (73/24)e^2 + (37/96)e^4](1 - e^2)^{-7/2}$ . For two black holes of  $M_{\text{BH,T}} = 10^6 M_{\odot}$  released during a galaxy merger on a circular orbit at a distance  $a \sim 10$  pc, this time far exceeds the age of the universe ( $t_{\text{GW}} \sim 10^{25}$  yr). It is thus clear that coalescing binary black holes are interesting astrophysical sources only if nature provides a dissipative mechanism that guides the inspiral from the scale of a merger, of  $\sim 100$  kpc, to the scale  $a_{\text{GW}}$  below which gravitational waves are conducive to coalescence on a timescale  $t_{\text{GW}} \lesssim 10^{10}$  yr: eq. (1) yields

$$a_{\text{GW}} = 2 \times 10^{-3} f(e)^{1/4} \frac{q_{\text{BH}}^{1/4}}{(1 + q_{\text{BH}})^{1/2}} \left( \frac{M_{\text{BH,T}}}{10^6 M_{\odot}} \right)^{3/4} \left( \frac{t_{\text{GW}}}{10^{10} \text{yr}} \right)^{1/4} \text{ pc} \quad (2)$$

corresponding to  $2 \times 10^4$  Schwarzschild radii for a black hole of mass  $M_{\text{BH,T}} = 10^6 M_{\odot}$ . At  $a_{\text{GW}}$ , the orbital period (for  $q_{\text{BH}} = 1$  and  $e = 0$ ) is of only

$$P(a_{\text{GW}}) = 2\pi \left( \frac{a_{\text{GW}}^3}{GM_{\text{BH,T}}} \right)^{1/2} \sim 5 \left( \frac{M_{\text{BH,T}}}{10^6 M_{\odot}} \right)^{5/8} \left( \frac{t_{\text{GW}}}{10^{10} \text{yr}} \right)^{3/4} \text{ yr} \quad (3)$$

and the relative circular velocity

$$V_{\text{cir}} = \left( \frac{GM_{\text{BH,T}}}{a_{\text{GW}}} \right)^{1/2} \sim 1742 \left( \frac{M_{\text{BH,T}}}{10^6 M_{\odot}} \right)^{1/8} \left( \frac{t_{\text{GW}}}{10^{10} \text{yr}} \right)^{-1/8} \text{ km s}^{-1} \quad (4)$$

is far in excess of the dispersion velocity of the ambient stars in a typical galaxy ( $\sim 100 - 300 \text{ km s}^{-1}$ ). The dynamic range for describing the hole's inspiral is so overwhelmingly large and extreme, going from the kpc scale down to  $a_{\text{GW}}$ , that a variety of processes may conspire to bring (or halt) the black holes down to (or away from) coalescence. Thus, the main focus of this review is to highlight the *physical* and *dynamical* processes that guide the sinking of massive black holes during binary mergers down to  $a_{\text{GW}}$ .

### 1.3 Dual, binary and recoiling AGNs in the realm of observations

Mergers occur either in gas-poor environments where collisionless/stellar processes are at play, or/and in gas-rich environments where gas-dynamical processes assist the black hole inspiral. Observations seem to reflect this dichotomy: accreting black hole pairs are seen in elliptical galaxies devoid of cold gas, as well as in ultra luminous infrared galaxies (ULIRGs), prototypes of gas-rich mergers between spirals. If accretion is triggered along the course of the merger, black holes can give origin to a rich phenomenology, that goes from dual to binary AGN activity, in the radio-loud or radio-quiete mode, according to their dynamics, habitat and merger type.

With *dual* AGNs we will indicate, in the following, dual black holes that are simultaneously active during a galaxy-galaxy encounter, but are still at large relative separations. In this case they are not physically bound in a binary and so, their dynamics is determined by the gravitational potential of the interacting

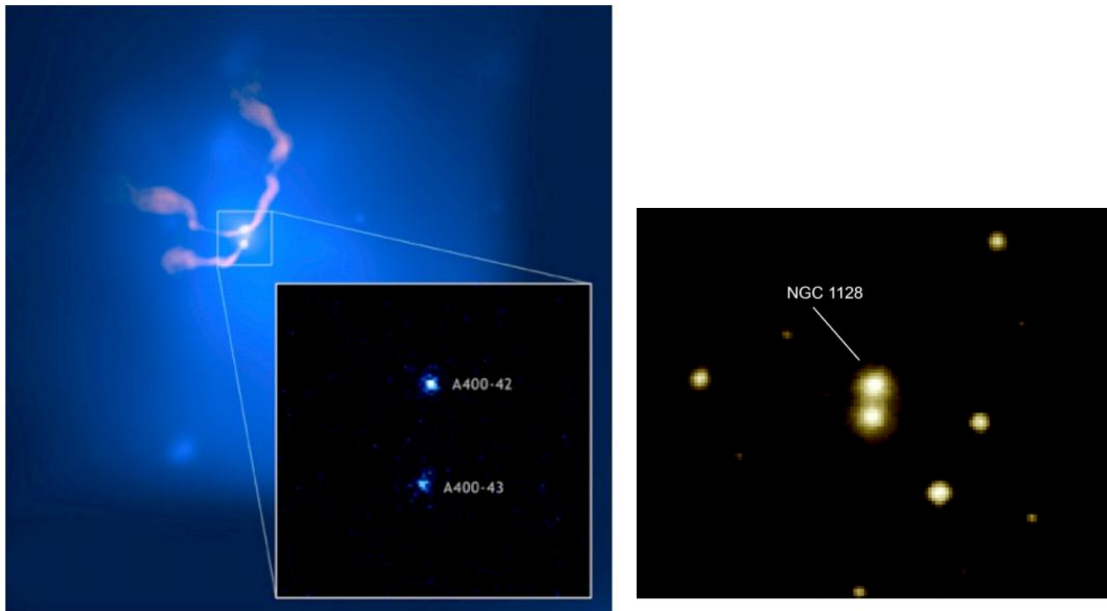


Figure 1: Composite X-ray (blue)/radio (pink) image of the galaxy cluster Abell 400 shows radio jets immersed in a vast cloud of multimillion degree X-ray emitting gas that pervades the cluster. The jets emanate from the vicinity of two supermassive black holes (bright spots in the X-ray enlarged image). These black holes are in the dumbbell galaxy NGC 1128 (whose optical image is on the right), which has produced the giant radio source, 3C 75.

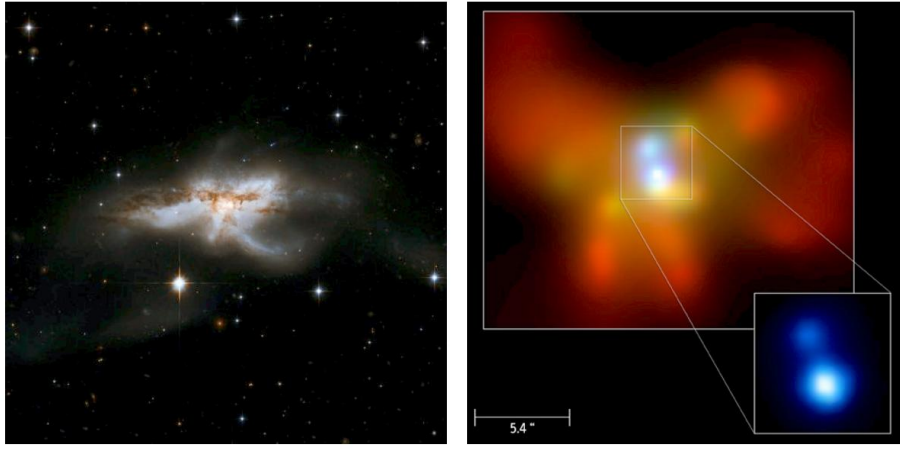


Figure 2: Optical image from *HST* (left). X-ray image<sup>58</sup> from *Chandra* (right) of the central region of NGC 6240 showing the presence of two active nuclei: red color refers to soft (0.5-1.5 keV), green to medium (1.5-5 keV), and blue to hard (5-8 keV) X-rays. 1'' corresponds to 700 pc in the galaxy. The AGN character of both nuclei is revealed by the detection of absorbed, hard, luminous X-ray emission and of two strong neutral Fe- $\alpha$  lines. Extended X-ray emission components are present, changing their rich structure in dependence of energy. The close correlation of the extended emission with the optical H- $\alpha$  emission of NGC 6240, in combination with the softness of its spectrum, clearly indicates its relation to star-burst-driven superwind activity.

system. With *binary* AGNs we will indicate active black holes that are at close enough distances that they form a Keplerian system in a merger remnant. *Recoiling* AGNs have been also hypothesized following the recognition that asymmetric gravitational wave emission leads to large recoil velocities: they should appear as off-center AGNs accreting from a small punctured disk<sup>45–47</sup>.

### 1.3.1 Dual AGNs

In our local universe, 3C 75 is a well studied double radio source at the center of the galaxy cluster Abell 400<sup>48–51</sup>. Figure 1 shows the radio and X-ray images of the composite source, and of the host galaxies in the optical. Evidence for interaction between the radio jets suggests that the sources are members of a system undergoing a large scale merger. *Chandra* observations have confirmed the presence of two X-ray nuclei 7 kpc apart, and of diffuse thermal emission along the radio streams, indicating that their proximity is not an artifact of a projection effect. 3C 75 is not the only case known of a dual AGN: PKS 2149-158 A and PKS 2149-158 B in Abell 2382 is a dumbbell system<sup>52</sup> hosting two radio cores with extended twin-jets, observed at a projected distance of 16 kpc. The jets emanate from two ellipticals of comparable luminosity and show signs of interaction with the intra cluster medium. Only through dedicated optical and X-ray follow-up observations it will be possible to prove that the underlying galaxies are in close physical interaction.

Dual AGNs have been recently discovered inside the dusty, obscured environment of at least two ULIRGs whose infrared emission is powered by an intense star-burst. The most compelling is the case of NGC 6240<sup>53–61</sup>, an on-going gas-rich merger between two spirals, shown in Figure 2: *Chandra* images have revealed that presence of two bright nuclear X-ray sources whose spectral energy distribution is consistent with being two accreting massive black holes (of 0.7 and  $2.4 \times 10^9 M_{\odot}$ <sup>59</sup>), seen at a projected distance of 700 pc<sup>61</sup>. Each nucleus is at the center of a stellar disk in rotation whose dynamics implies the presence of more than  $10^9 M_{\odot}$  of stars<sup>57</sup>. Kinematic evidence exists that the two nuclei are not physically bound yet, and that the system is caught in the immediate proximity of its first close passage. A massive rotating disk of cold gas together with gas filaments fill the space in between the two active nuclei<sup>57</sup>. Mrk 463 is the second case<sup>62</sup>: this ULIRG shows clear morphological signs of an interaction between two gas-rich galaxies, and two luminous obscured X-ray nuclei are observed at a projected distance of 3.8 kpc. The interacting star-burst system Arp 299 is a potential third candidate of a dual AGN<sup>63–67</sup>, due to the presence of a highly obscured X-ray nucleus (in the galaxy member NGC 3690) and possibly of a second less luminous one (in IC 694), at a projected distance of 4.6 kpc. Dynamical mass estimates indicate that the black holes in Arp 299 are nested in massive ( $\gtrsim 10^9 M_{\odot}$ ) nuclear gaseous disks of  $\lesssim 50$  pc in size.

While the above cases refer to dual AGNs in galaxies of comparable mass (i.e. major mergers), dual AGNs in minor merger are still difficult to observe. Despite this, a system of two offset nuclei has been discovered in the disturbed disk galaxy NGC 3341. The two offset nuclei have projected distances of 5.1 and 8.4 kpc from the primary center<sup>68</sup>. One of the two offset nuclei (object B) shows a Seyfert 2 spectrum, typical of an accreting black hole. This unusual system, shown in Figure 3, can be viewed as a minor merger in action with two dwarf galaxy satellites falling onto the more massive primary. As the primary nucleus indicates a possible low-level of AGN activity typical of a LINER, NGC 3341 may be the first candidate dual AGN system in a composite, triple minor merger.

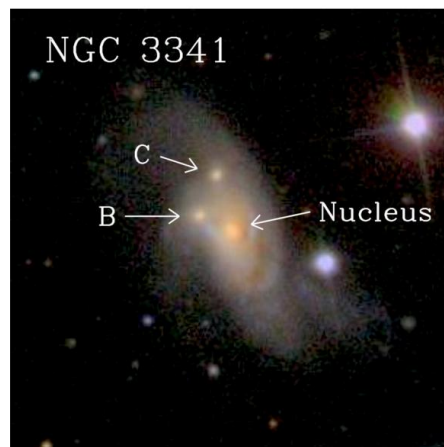


Figure 3: SDSS color-composite image of NGC 3341 in the field of view of  $2' \times 2'.68$ . NGC 3341 is a disturbed disk galaxy undergoing a minor merger with two dwarf companions. Objects B and C are located at projected separations of  $9.5''$  and  $15.6''$  (5.1 and 8.4 kpc) from the primary nucleus. Object B hosts an active nucleus.



### 1.3.2 Binary or recoiling AGNs

The existence of binary AGNs is still debatable at observational level, and four cases deserve attention. The first refers to the elliptical galaxy 0402+379<sup>69–72</sup>. VLBI (high spatial resolution) observations have offered the view of two compact flat-spectrum radio sources C1 and C2 at a projected separation of only 7 pc<sup>70</sup>. Two jets depart from C1, while C2 (initially interpreted as a bright knot along one jet) shows signs of variability that are a distinguishing feature of an active black hole. Thus, two massive black holes are powering the radio-emission, and are likely to form a real *binary* in a passively evolving elliptical.

The second is the case of OJ 287, a BL Lac object present on photographic plates since 1891. Its complex optical light curve shows a periodic variation of  $\sim 12$  yr suggesting that the engine is a massive binary black hole with the smaller (secondary) orbiting the larger hole with an observed 12 yr orbital period<sup>73–75</sup>. Maximum brightness is obtained when the secondary black hole, moving on an inclined orbit, plunges into the accretion disk that surrounds the primary; a second enhancement in brightness is detected a year later, interpreted as perturbed gas falling onto the primary. For OJ 287, the primary (secondary) black hole has an estimated mass of  $2 \times 10^{10} M_{\odot}$  ( $2 \times 10^8 M_{\odot}$ ) implying an orbital decay timescale via emission of gravitational radiation of only  $\gtrsim 10^5$  yr.

The third candidate is the quasar SDSS 092712.65+294344<sup>76</sup>. No periodicities in the light curve are observed in this source, but a systematic shift of  $2650 \text{ km s}^{-1}$  in its composite set of emission lines. SDSS 092712.65+294344 has been presented in literature as first case of recoiling black hole<sup>77</sup>: in this interpretation, the set of very narrow emission lines at the redshift of the galaxy host result from illumination of central gas by the active black hole. Moving with line-of-sight speed of  $2650 \text{ km s}^{-1}$  away from the galaxy core, the black hole that drags its own accretion disk is responsible of the blue-shifted broad line emission resulting from gas clouds bound to the black hole itself. This picture is challenged by the presence, in the optical spectrum, of a third set of narrow lines at the same redshift of the broad line system which do not find a clear-cut interpretation. In the recoiling hypothesis, tenuous gas moving with the black hole is responsible to the emission. However, to a closer scrutiny, this quasar offers at least two alternative interpretations. SDSS 092712.65+294344 may host a binary whereby a secondary (lighter) black hole, orbiting around a more massive primary, is fed by matter flowing from a circum-binary disk in close tidal contact<sup>78,79</sup>. In this picture, the narrow lines that define the rest frame galaxy would still result from the central illumination offered by the binary, the broad line blue-shifted set from gas clouds bound to the orbiting secondary, and the narrow blue-shifted lines from rarefied gas around the secondary black hole that has excavated a gap in the surrounding disk (as described in Section 5.4). Under this hypothesis, the mass of the primary has been estimated  $\sim 2 \times 10^9 M_{\odot}$ , the mass ratio between the two black holes  $\sim 0.3$ , and an orbital semi-major axis  $\sim 0.34$  pc, corresponding to an orbital period of 340 yr and  $t_{\text{GW}} \sim 3 \times 10^9$  yr. The binary hypothesis is preferred over the recoiling hypothesis being one hundred times more probable than the ejection hypothesis<sup>79</sup>. Furthermore, it can be directly tested by searching for systemic Doppler changes in the velocity due to orbital motion<sup>78</sup>. A third alternative is that SDSS 092712.65+294344 is the composite system of two active AGNs co-present inside two galaxies that are in the verge of colliding at high relative speed in a galaxy cluster<sup>80,81</sup>.

The four and last candidate is the quasar SDSS J153636.22+044127.0<sup>82</sup> discovered recently in a systematic search of quasars with anomalous spectra, among 17.500 sources with redshift  $\lesssim 0.7$  in the SDSS DR7 release. The quasar shows two clear broad line emission systems separated in velocity by  $3500 \text{ km s}^{-1}$ , plus a third unresolved absorption line system at an intermediate velocity (interpreted as emission from intervening

material along the line of sight). Boronson & Lauer<sup>82</sup> interpreted this object as a binary system of two black holes with their own emission line system.<sup>1</sup>

## 1.4 The quest for massive black hole binaries in ellipticals

Elliptical galaxies are believed to be the end product of multiple mergers<sup>83–85</sup>, though the exact sequence of events that shape ellipticals as they appear today is still uncertain. Ellipticals show remarkable regularities in their smooth stellar light profile: their outer surface brightness  $I(r)$  follows a Sérsic profile  $\log I(r) \propto r^{1/n}$  over a wide mass-dynamical range. The fit is so remarkable that departures from this regularity has been recently used as diagnostic tool for tracing back their formation history<sup>86</sup>.

Ellipticals appear to come in two distinct varieties<sup>86,87</sup>: bright (giant) ellipticals have Sérsic index  $n > 4$  and show cores, i.e. *missing-light* inside a radius marking the dividing line between a flatter inner surface brightness profile and the Sérsic profile at outer radii; the less bright, less massive (normal) ellipticals have instead  $n \lesssim 4$ , and show *extra-light* at their center relative to the inner extrapolation of the outer Sérsic profile. Missing or extra light are features that underscore a dichotomy that involves not only the central kpc of the galaxy but many global structural and physical properties<sup>88</sup>. Core (i.e. missing-light) giant ellipticals are essentially non-rotating, anisotropic and modestly triaxial; stars are very old and if gas is present, it is *hot* and X-ray emitting. Often giant ellipticals host strong radio sources. By contrast, core-less (i.e. extra-light) ellipticals are rotationally supported and have disky-distorted isophotes. Rarely contain hot X-ray emitting gas and a radio source. Both local and global features thus appear to record memory of a different merger history. A number of authors<sup>86,89,90</sup> has suggested recently that missing-light (giant) ellipticals are shaped by (re-)mergers of *gas-poor* galaxies, while extra-light ellipticals are the result of a *gas-rich* merger producing an extra stellar component in the central regions of the galaxy<sup>89</sup>. Extra-light in normal ellipticals is suggestive that *cold* gas has played a critical role in the build up of the galaxy: gas can radiate and fall in the central regions of the merger remnant converting a sizable fraction of its mass into stars, in violation of Liouville’s theorem. Missing light<sup>90</sup> instead does not find an easy explanation: collisionless mergers preserve the density profile of the progenitor galaxies and do not enhance significantly the velocity dispersion, according to Liouville’s theorem. Thus, the presence of missing-light requires extra physics.

Core (missing-light) galaxies and core-less (extra-light) ellipticals generally host a massive black hole in their nucleus, and an interesting hypothesis has been advanced. That in a gas-poor environment, missing-light results from a dynamical process involving a *binary* black hole. A first possibility is that a stellar core forms in response to repeated three-body interactions between the binary and a star passing by<sup>91</sup>: impinging on the binary from low angular momentum orbits stars are scattered back with very high velocities and leave the nucleus. The binary that decays excavates with time the central region of the galaxy producing a stellar core, emptied of light. The missing light correlates with the black hole mass closely<sup>87,92,93</sup> and with the number of successive mergers necessary to explain the stellar mass deficit<sup>93,94</sup>. A second possibility that

---

<sup>1</sup>After submission of this review, new observations, in the optical and radio bands, are hinting for interpretations alternative to the binary black hole hypothesis. Chornock et al. (arXiv:0906.0849) ascribe the peculiar features of this quasar to a single massive black hole with properties common to the class of double-peaked emitters. Wrobel and Laor (arXiv:0905.3566) observed SDSS J1536+0441 using VLA discovering two radio sources separated by 5 kpc within the quasar optical localization region. Decarli et al. (ATel n.2061) and Lauer and Boronson (arXiv:0906.0020) discovered the presence of a companion galaxy in correspondence of the second radio source, and most recently, Decarli et al. (submitted to ApJL) found evidence that the quasar lives in a galaxy cluster. These observations leave open the possibility that the source is a dual quasar, and only through high angular-resolution spectroscopy, it will be possible to disentangle the nature of SDSS J1536+0441.

may operate in succession is core formation due to the recoiling black hole born after binary coalescence. Gravitational radiation not only carries away energy and angular momentum: depending on the black hole spin direction relative to the orbital plane, radiation transports away linear momentum, as waves are emitted anisotropically. The relic black hole, as already mentioned in Section 1.2, receives a recoil velocity that can be as large as  $4000 \text{ km s}^{-1}$ . The instantaneous removal of the black hole via radiation recoil generally results in the rapid formation of a stellar core that expands due to the sudden change in the gravitational potential, now lacking of a massive central body, and to the subsequent deposition of kinetic energy as the black hole returns toward the center of the galaxy<sup>95–97</sup> (the effect being the largest when the hole is ejected on a return orbit with a velocity just below escape). These ideas radical and ad hoc have become nowadays two mainstream possibilities.

But, how can core excavation be prevented in core-less ellipticals? A possibility is that gas has played a critical role not only in creating new additional light but in accelerating binary decay (if a binary is present) under the action of gas-dynamical torques. The working hypothesis is that fast orbital decay controlled by gas prevents core formation; spin-orbit alignment which is favored in a gas rich environment<sup>98</sup>, brings the two holes in a configuration, prior to coalescence, of minimum recoil, thus preventing expansion of the stellar core at the time of formation of the new, relic hole.

From the above considerations, black hole binaries seem to be linked in fundamental ways to the dynamics of the stellar and gas components of galaxies, and this motivates strongly the interest on binary black holes not only as sources of gravitational waves, but as key systems in the context of galaxy formation.

## 2 Black hole dynamics in galaxy mergers

Mergers occur mainly in two varieties: they may involve nearly equal mass galaxies, and these are referred to as *major* mergers, or unequal mass galaxies, i.e. *minor* mergers. Both may involve either gas-rich or gas-poor galaxies so that black hole dynamics has no unique outcome but differs in relation to the merger type and environment. Exploring these diversities in a self-consistent cosmological scenario is currently a challenge, and thanks to recent advances in numerical simulations, it is now possible to address a number of compelling issues. Galaxy mergers cover cosmological volumes ( $\lesssim 100 \text{ kpc}$  aside), whereas black hole coalescences probe exceedingly small volumes from  $\lesssim 1 \text{ pc}$  down to  $a_{\text{GW}} \sim 10^{-3} \text{ pc}$  and to the horizon scale ( $10^{-7} \text{ pc}$ , for  $\sim 10^6 M_{\odot}$ ). Thus, tracing the black hole inspiral in a merger requires simulations with gravitational/hydrodynamical force resolution covering more than ten orders of magnitude in length, and a variety of different physical processes, often not scale free.

Following a merger, how can black holes reach the gravitational wave inspiral regime? The overall scenario has first been outlined in a seminal study by Begelman, Blandford & Rees<sup>99</sup>, in the context of stellar systems. Four main phases characterize the dynamical evolution of the black holes: (I) the pairing phase P in which dynamical friction against the stellar/dark matter background is acting on each black hole causing their sinking; (II) phase B when the holes dynamically couple to form a *binary* and continue to sink due to the large scale drag of dynamical friction; (III) phase H in which the binary hardens via 3-body scatterings off single stars; (IV) phase GW, the last, when gravitational wave back-reaction becomes important to drive the inspiral down to coalescence.

Early studies explored the phase of pairing P, simulating the collisionless merger of spherical halos<sup>100,101</sup>. Governato, Colpi & Maraschi<sup>100</sup> in particular first noticed that when two equal mass halos merge, the twin

black holes nested inside the more massive nuclei are dragged rapidly toward the center of the remnant and form a close pair. The drag, initially, is not acting on the individual holes but on the massive stellar-cusp in which they are hosted. Only when the merger is in its advanced stage, the black holes behave as independent point masses and continue to lose orbital angular momentum under the action of dynamical friction. They further noticed that the situation reverses in unequal mass (minor) mergers, where the less massive halo, tidally disrupted along the course of the encounter, leaves its *naked* black hole wandering in the outskirts of the main halo. Thus, depending on the halo mass ratio and internal structure of the interacting galaxies, the transition from phase P  $\rightarrow$  B can be at some point prematurely aborted or severely delayed. Similarly, the transit from phase B  $\rightarrow$  H  $\rightarrow$  GW is not always secured even in major mergers (where also the black holes are expected to have comparable masses), as the stellar content in the immediate vicinity of the black holes may not suffice to harden the binary down to a separation where gravitational wave driven inspiral sets in<sup>101–104</sup>. All these issues will be discussed critically below.

N-Body and Monte Carlo merger trees simulations<sup>105–113</sup> describing the assembly of galaxies show that unequal mass mergers are common along cosmic history. As black hole masses, in the local universe, correlate tightly with the mass of the host<sup>1–4</sup> ( $M_{\text{BH}} \sim 10^{-3} M_{\text{halo}}$ ), this implies a black hole mass spectrum ranging from  $10^5 M_{\odot}$  up to  $10^9 M_{\odot}$  and mass ratios  $q_{\text{BH}} \sim 0.01–1$ . In literature, these intervals have not been explored systematically and main emphasis has been given to equal-mass mergers, given the heavy computational demand, and the impossibility, in gas-rich mergers, of using self-similar solutions, owing to the presence of dissipative components. While black hole masses in the interval  $10^5 – 10^7 M_{\odot}$  are of interest for *LISA* astrophysics, black holes with  $M_{\text{BH}} > 10^8 M_{\odot}$  are of key importance for the Pulsar Timing Array Experiment (PTA), due to their different frequency of operation. While the "light" *LISA* black holes carry information on how/where they formed along the course of galaxy assembly<sup>110</sup> (up to  $z \sim 20$ ), the "heavy" PTA black holes<sup>34</sup> trace mergers among very massive galaxies present in the already evolved universe, at redshift  $z \lesssim 1$ .

## 2.1 Capturing basic physics

### 2.1.1 Dynamical friction

Dynamical friction is the main cause of braking of the black hole orbits during the process of pairing, and acts individually on each hole. This drag arises in response to the gravitational perturbation excited by the black hole on the background of dark matter and/or stars. In the original formulation of Chandrasekhar<sup>114</sup>, the drag is the collective result of momentum exchange between the massive perturber  $M_{\text{BH}}$  (the black hole in our case) and every single particle of the background. In a collisionless system of uniform mass density  $\rho_*$  and isotropic velocity distribution, the force on  $M_{\text{BH}}$ , acting against its velocity vector  $\mathbf{V}$  is

$$\mathbf{F}_{\text{DF}} = -4\pi \ln \Lambda G^2 M_{\text{BH}}^2 \rho_* \left[ \text{erf} \left( \frac{V}{\sqrt{2}\sigma} \right) - \left( \sqrt{\frac{2}{\pi}} \frac{V}{\sigma} \right) \exp \left( -\frac{V^2}{2\sigma^2} \right) \right] \frac{\mathbf{V}}{V^3}. \quad (5)$$

The gravitational drag that involves only those particles moving more slowly than  $V$  (the term in squared brackets), is maximum when the velocity  $V$  of the perturber nears the 1D velocity dispersion  $\sigma$ , as the force declines linearly with  $V$ , and as  $V^{-2}$ , in the low ( $V \ll \sigma$ ) and high ( $V \gg \sigma$ ) speed limit, respectively. The Coulomb logarithm  $\ln \Lambda \sim \ln(b_{\text{max}}/b_{\text{min}})$  in equation (5) expresses the non-locality of the drag as it comprises the whole range of impact parameters relevant for the exchange of momentum in the interaction of the stars with  $M_{\text{BH}}$ . Since gravity is a long-range force,  $b_{\text{max}}$  is close to the size  $L$  of the collisionless background, while  $b_{\text{min}} = V^2/GM_{\text{BH}}$  is the impact parameter for a large-scattering angle gravitational

interaction. Dynamical friction expresses the tendency of gravitating systems to reach energy equipartition, so that any excess of kinetic energy (that carried by the hole) is distributed among all particles. Restricted to a static, infinite, isotropic and homogeneous collisionless medium, Chandrasekhar's formula assumes that the stars/dark-matter particles move along unperturbed trajectories that are straight lines, thus neglecting the self-gravity present in real backgrounds. Despite this limitation, the formula has been often used to estimate sinking times also in inhomogeneous self-gravitating backgrounds evaluating  $\rho_*$  and  $\sigma$  at the current, i.e. local position of the perturber, treating  $\ln \Lambda$  as adjustable parameter.

Many approaches has been developed to overcome the limits of the local approximation, including the theory of linear response TLR<sup>115,116</sup>. In TLR, dynamical friction is viewed as a direct manifestation of the fluctuation-dissipation theorem<sup>117,118</sup>. In this interpretation, the fluctuations of the two-body force between the massive perturber  $M_{\text{BH}}$  and any particle  $m_*$  add collectively to give a non-vanishing drag. In a medium characterized by a distribution function  $f(\mathbf{r}, \mathbf{p})$ , the components of the force can be expressed as the sum over time and phase-space  $(\mathbf{r}, \mathbf{p})$

$$F_{\text{TLR}}^a = G^2 M_{\text{BH}}^2 \int_{-\infty}^t ds \int d_3\mathbf{r} d_3\mathbf{p} \frac{\partial f}{\partial p^b} T^{ba} \quad (6)$$

of a suitable self-correlation tensor

$$T^{ba} = Nm_*^2 \frac{r_{\text{BH}}^b(s) - r^b}{|\mathbf{r}_{\text{BH}}(s) - \mathbf{r}|^3} \frac{r_{\text{BH}}^a(t) - r^a(t-s)}{|\mathbf{r}_{\text{BH}}(t) - \mathbf{r}(t-s)|^3} \quad (7)$$

correlating the two-body gravitational force between the black hole (in  $\mathbf{r}_{\text{BH}}$ ) and any individual star (in  $\mathbf{r}$ ) at time  $t$  with that at the earlier time  $(t-s)$ . This formula captures the complexity of the physics leading to the orbital decay of a mass  $M_{\text{BH}}$  in a generic self-gravitating background. The drag force at time  $t$  keeps *memory* of the previous history of the composite system, as its strength depends on the dynamics of the perturber and of the particles at earlier times as determined by the unperturbed Hamiltonian. Applied to selected spherical environments<sup>116</sup>, TLR has been powerful to prove that the stellar response embodied in  $T^{ba}$  remains correlated with the perturbation for a time shorter than the typical orbital time of stars and that the force arises preferentially from those stars closer to the perturber, due to the inhomogeneity of the background (distant lower density regions contribute less to the drag). Tested against high resolution numerical simulations<sup>116</sup>, TLR has been useful also in showing that in the interplay between loss of energy and angular momentum, eccentric orbits do not circularize under the action of the drag force, but remain eccentric along the course of the decay implying shorter sinking times. In a singular isothermal sphere with 1D velocity dispersion  $\sigma$  and density profile  $\rho(r) = \sigma^2/[2\pi Gr^2]$ , TLR predicts a sinking time, expressed in terms of the circularity  $\epsilon$  (defined as the ratio between the angular momentum of the current orbit relative to that of a circular orbit of equal energy)

$$\tau_{\text{DF}} = 1.2 \frac{r_{\text{cir}}^2 V_{\text{cir}}}{\ln(M_{\text{halo}}/M_{\text{BH}}) GM_{\text{BH}}} \epsilon^{0.4}, \quad (8)$$

where  $r_{\text{cir}}$  and  $V_{\text{cir}}$  are the initial radius and velocity of the circular orbit with the same energy of the actual orbit, and  $M_{\text{halo}}$  is the mass of the dark matter and stars within  $r_{\text{cir}}$ . Equation (8) indicates that a massive black hole can sink at the center of the sphere within a time  $\sim 10^8$  yr, if released during the merger at a distance of  $\sim 100$  pc:

$$\tau_{\text{DF}} \sim 5 \times 10^8 \left( \frac{5}{\ln[M_{\text{halo}}/M_{\text{BH}}]} \right) \left( \frac{r_{\text{cir}}}{300 \text{pc}} \right)^2 \left( \frac{V_{\text{cir}}}{\sqrt{2} \times 100 \text{km s}^{-1}} \right) \left( \frac{10^6 M_{\odot}}{M_{\text{BH}}} \right) \epsilon^{0.4} \text{yr}. \quad (9)$$

Dynamical friction acts also in collisional fluids and arises again from the gravitational pull between the perturber and its density wake excited in the ambient medium. In the steady-state limit and for *supersonic* motion, the drag on a massive perturber moving with velocity  $\mathbf{V}$  across a homogeneous fluid with density  $\rho_{\text{gas}}$  and sound speed  $c_s$  reads

$$\mathbf{F}_{\text{DF}}^{\text{gas}} = -4\pi \ln \left[ \frac{b_{\text{max}} (\mathcal{M}^2 - 1)^{1/2}}{b_{\text{min}} \mathcal{M}} \right] G^2 M_{\text{BH}}^2 \rho_{\text{gas}} \frac{\mathbf{V}}{V^3}, \quad \text{for } \mathcal{M} > 1 \quad (10)$$

where  $\mathcal{M} = V/c_s$  is the Mach number. The deceleration results, in this regime, by the enhanced density wake that lags behind the perturber and that is confined in the narrow cone, the Mach cone, whose surfaces of constant density are hyperboloids<sup>119</sup>. The main result is that the gaseous drag is enhanced for supersonic motion (with  $\mathcal{M} \sim 1 - 2.5$ ) compared to Chandrasekhar's formula (for  $\rho_* = \rho_{\text{gas}}$ ) by a factor  $\sim 2$  hinting for shorter timescales when dynamical friction occurs in gaseous backgrounds<sup>119</sup>. A black hole can also accrete while sinking and a drag, comparable in strength to the large-scale force  $\mathbf{F}_{\text{DF}}^{\text{gas}}$  arises due to accretion:  $\mathbf{F}_{\text{BHL}}^{\text{gas}} = -\dot{M}_{\text{B}} \mathbf{V}$  where  $\dot{M}_{\text{B}}$  is the Bondi-Hoyle-Littleton accretion rate so that

$$\mathbf{F}_{\text{BHL}}^{\text{gas}} = -4\pi \lambda G^2 M_{\text{BH}}^2 \frac{\rho_{\text{gas}}}{(V^2 + c_s^2)^{3/2}} \mathbf{V} \quad (11)$$

(with  $\lambda \lesssim 1$ ), valid for any  $\mathcal{M}$ .

The *subsonic* case is instead more elusive, because sound waves can propagate both down-wind and up-wind so that the drag, in this low speed limit, can be much weaker than in the collisionless case. The drag is exactly zero in a homogeneous infinite medium due to the front-back symmetry of the perturbed density distribution present in any stationary solution. However this result does not rigorously hold if one performs a finite time analysis<sup>119</sup>. If the perturber triggers the disturbance at time  $t = 0$  and moves subsonically along a straight line, the symmetry is broken as long as  $(c_s + V)t$  is smaller than the size of the medium, resulting in a finite drag  $\mathbf{F}_{\text{DF}}^{\text{gas}} = -(4/3)\pi G^2 M_{\text{BH}}^2 \rho_{\text{gas}} \mathcal{M}^3 \mathbf{V}/V^3 \propto M_{\text{BH}}^2 \rho_{\text{gas}} \mathbf{V}/c_s^3$  for  $\mathcal{M} \ll 1$ .

Equations (5-11) set the guidelines for our understanding of dynamical friction. As the drag  $F_{\text{DF}}$  is proportional either to  $\rho_*$  or  $\rho_{\text{gas}}$ , black holes find their preferred way toward coalescence in backgrounds as those created in dissipative mergers. Gas can play an important role there: subject to instabilities and shocks, it can cool and control preferentially the inspiral creating conditions were  $\rho_{\text{gas}} > \rho_*$ .  $F_{\text{DF}}$  is also a sensitive function of  $V/\sigma$  or  $\mathcal{M} = V/c_s$  and is large when  $V/\sigma$  and/or  $\mathcal{M} \sim 1$ . Nevertheless, this basic formulation can not capture important details of the process. In a real merger:

- The underlying gravitational field is fluctuating violently;
- Prior to the encounter, the black holes are often inside massive power-law stellar cusps and thus have effective mass  $M_{\text{BH,eff}}$  larger than their own mass;
- Tides strip stars in the cusp and  $M_{\text{BH,eff}}$  changes long the course of the merger, as  $M_{\text{BH,eff}} \rightarrow M_{\text{BH}}$ ;
- Stars and gas are co-present, but often have different geometries and so, they respond differently to the perturbation induced by the black hole: in rotating backgrounds the gravitational pull of  $M_{\text{BH}}$  creates spiral patterns that can not simply be described by a back-stream density wake;
- The density wakes excited by the two black holes may start to self-interact and overlap as the hole's separation decreases.
- When the process of pairing under dynamical friction is sufficiently advanced, the black holes form a binary, and at this stage the interaction changes character. In presence of a collisionless (stellar) background, it is

the interaction of individual stars that drives binary evolution, while in a collisional fluid, gravitational and viscous torques play a key role.

- The black holes may start to inject energy and momentum in the medium modifying the underlying density, and in turn the back-reaction force on their orbit.

### 2.1.2 From Pairing to Hardening: key scales

If, in the simplest approximation, the collisionless background is described as a singular isothermal sphere, two black holes form a binary when their separation  $a$  falls below the distance  $a_{\text{binary}}^*$  at which the mass in stars/dark matter enclosed within their relative orbit is equal to the total mass  $M_{\text{BH,T}}$  of the binary:

$$a_{\text{binary}}^* \sim \frac{GM_{\text{BH,T}}}{2\sigma^2} \sim 0.2 \left( \frac{M_{\text{BH,T}}}{10^6 M_{\odot}} \right) \left( \frac{100 \text{ km s}^{-1}}{\sigma} \right)^2 \text{ pc.} \quad (12)$$

At  $a \sim a_{\text{binary}}^*$ , the hole's relative circular velocity equals the circular velocity of the stars,  $\sqrt{2}\sigma$ . Dynamical friction continues to drive the inspiral, but as soon as  $V_{\text{cir}}$  increases above  $\sqrt{2}\sigma$ , the interaction between the binary and the stars from collective becomes individual, and the drag no longer shows the clear dependence on  $M_{\text{BH,T}}$ . *Scattering off the binary by single stars* becomes the main process for extracting binding energy and angular momentum from the orbit. When a star is impinging on the binary, it is shot out at an average velocity comparable to the binary's orbital velocity  $V_{\text{cir}}$  (eq. 4). If  $V_{\text{cir}}$  exceeds the 3D velocity dispersion  $\sqrt{3}\sigma$ , stars are ejected away from the galaxy nucleus with very high speeds, and this occurs as soon as the binary reaches the hardening radius<sup>120</sup>, defined as the binary separation at which the binding energy per unit mass exceeds  $(3/2)\sigma^2$ :

$$a_{\text{hard}}^* = \frac{G\mu_{\text{BH}}}{3\sigma^2} \sim 0.13 \frac{q_{\text{BH}}}{(1+q_{\text{BH}})^2} \left( \frac{M_{\text{BH,T}}}{10^6 M_{\odot}} \right) \left( \frac{100 \text{ km s}^{-1}}{\sigma} \right)^2 \text{ pc.} \quad (13)$$

Below  $a_{\text{hard}}^*$ , stars leave the galaxy's core carrying away a tiny fraction of the binary energy, approximately  $\sim (3/2)Gm_*\mu_{\text{BH}}/a$ , where  $\mu_{\text{BH}} = M_{\text{BH,T}}q_{\text{BH}}/(1+q_{\text{BH}})^2$  is the reduced mass of the binary<sup>120</sup>. This corresponds to an increase of the binary's binding energy  $E_{\text{B}}$  and thus a decrease in the semi-major axis per scattering of the order of  $\delta a/a = \delta E_{\text{B}}/E_{\text{B}} \sim m_*/M_{\text{BH,T}}$ .

According to this loss, the binary continues to harden transiting from B  $\rightarrow$  H, and from H  $\rightarrow$  GW, and to accomplish this, it needs to eject a mass in stars

$$M_{\text{ej}} \sim \frac{1}{3}\mu_{\text{BH}} \ln \left( \frac{a_{\text{hard}}^*}{a_{\text{GW}}} \right) \sim (10 - 20)\mu_{\text{BH}} \quad (14)$$

for a typical galaxy's nucleus<sup>120,121</sup>. Whether the binary will eject this mass, and complete the inspiral down to the gravitational wave domain will be discussed in Section 3.

If the black holes move inside the gaseous background of a nuclear disk that forms in a merger, we can introduce the scale below which they bind  $a_{\text{binary}}^{\text{gas}}$ : to this purpose, we consider as reference model a Mestel disk, i.e. a rotationally supported, self-gravitating disk characterized by a surface mass density profile  $\Sigma = \Sigma_0(R_0/R)$  where  $R$  is the projected radial distance and  $\Sigma_0$  the density at the scale radius  $R_0$ . The disk,

in differential rotation  $\Omega_{\text{disk}}(R) = V_{0,\text{rot}}/R$  with constant  $V_{0,\text{rot}}$ , has a total mass  $M_{\text{disk}} = 2\pi\Sigma_0 R_0^2$ . The black holes form a binary whenever the disk mass enclosed within  $a$  equals  $M_{\text{BH,T}}$ :

$$a_{\text{binary}}^{\text{gas}} = R_0 \frac{M_{\text{BH,T}}}{M_{\text{disk}}} \sim 1 \left( \frac{R_0}{100 \text{ pc}} \right) \left( \frac{M_{\text{BH,T}}}{10^6 M_\odot} \right) \left( \frac{10^8 M_\odot}{M_{\text{disk}}} \right) \text{ pc.} \quad (15)$$

In a fluid, the binary does not interact with an isolated parcel of gas since any perturbation is transmitted to the fluid either via shocks or through acoustic waves. Thus, below  $a_{\text{binary}}^{\text{gas}}$  the interaction remains collective. In the transit from B  $\rightarrow$  H  $\rightarrow$  GW, the binary continues to exchange angular momentum with the gas and to deposit energy that can be radiated away, in a manner that will be described in Section 5.

A key radius that can be introduced to describe the coupling of the black hole with its environment, is the gravitational influence or Bondi-Hoyle-Littleton radius

$$R_{\text{BHL}} \sim \frac{GM_{\text{BH}}}{(c_s^2 + V_{\text{rel}}^2)} \sim 0.4 \left( \frac{M_{\text{BH}}}{10^6 M_\odot} \right) \left( \frac{(100 \text{ km s}^{-1})^2}{c_s^2 + V_{\text{rel}}^2} \right) \text{ pc} \quad (16)$$

(where  $V_{\text{rel}}$  is the velocity of the black hole relative to the medium) that indicates the size of the region of dynamical influence of each black hole on fluid particles. Thus, as soon as the binary separation drops below  $R_{\text{BHL}}$ , the gravitational field of both holes is expected to affect the geometry, dynamics and thermal state of the gas, and key physical processes for black hole inspiral will be described in Section 5.

## 2.2 Capturing basic physics from key numerical experiments

Figure 4 shows the result of a study by Milosavljevic & Merritt<sup>101</sup> who simulated the idealized merger of two identical spherical galaxies with twin black holes, combining the tree code GADGET<sup>122</sup>, used as integrator to trace the early stages of the merger when the black holes are subject to dynamical friction in the pure stellar background, to the code NBODY6++<sup>123</sup>, a direct-summation N-Body code that follows the dynamics of the black holes scattering off individual stars, in the advanced stages of the merger. As illustrated in Figure 4 (upper panel, first row) the black holes initially remain closely associated with their stellar cusp. In this phase black hole pairing is controlled by dynamical friction which is acting not only on the individual black holes but on the black hole+star’s cusp system. As time proceeds, the two cusps merge into a regenerated cusp with density comparable to the initial, and the black holes form a binary (second row). In the last two rows, the interaction of the binary with the stars is no longer collective and is followed with the direct-summation N-Body code. Dynamical friction plays no role, and three-body scattering becomes the main process of binary hardening that continues at a different pace. Meantime, stars are ejected and core scouring starts. This is illustrated again in Figure 4 (last two rows) where the density of the newly-formed cusp continues to drop as the black hole binary transfers energy to the stars. The code NBODY6++ can not follow however the *long-term* evolution of the binary as a variety of spurious collisional effects, associated to the small number of particles  $N$  used, leads to an unphysical, rapid decay of the binary. Because of the numerical discreteness effects associated with approximating a galaxy nucleus with  $N \gtrsim 10^9 - 10^{10}$  stars by a model consisting at best of  $N \gtrsim 10^6$  particles, direct N-Body simulations appear to be limited to the early stages of phase H. For this reason the subsequent evolution will be described in Section 3.

As far as gas-drag is concerned, Figure 5 shows a case-study by Escala et al.<sup>124</sup> who simulated using GADGET in its SPH implementation, the sinking of two black holes in a spherical isothermal gas cloud. The black



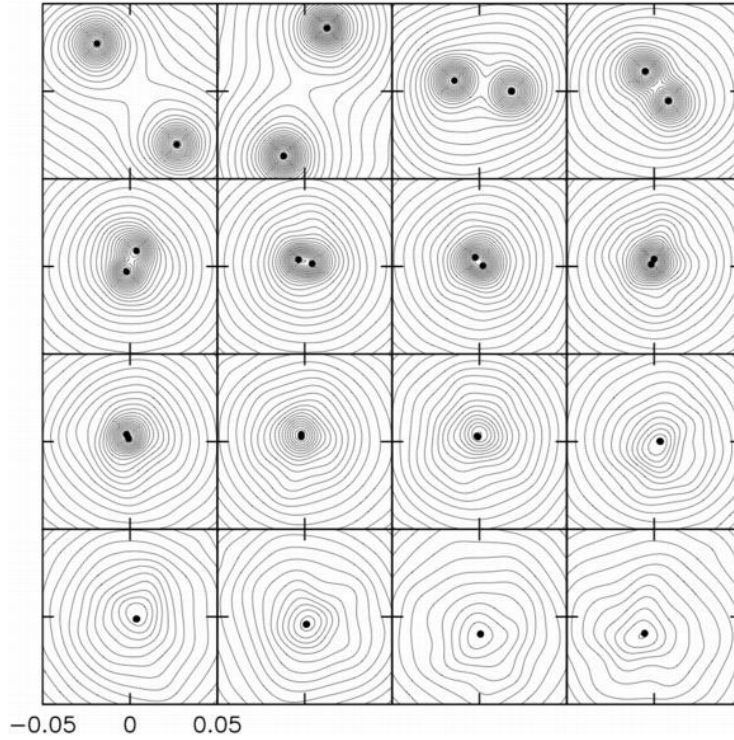


Figure 4: Projected density contours describing the merger of twin spherical stellar systems set initially on an elliptical orbit<sup>101</sup>. The two black holes (filled circles) of total mass  $M_{\text{BH,T}} = 0.01M_{\text{galaxy}}$  are at the center of the two stellar cusps that spiral-in under the influence of dynamical friction (first row). The two cusps merge (in second row) and the black holes form a binary inside a newly regenerated stellar cusp whose profile is close to the initial profile. Three-body scatterings of single stars cause the progressive hardening of the binary and the excavation of a stellar core as stars are ejected above escape velocity. The density of the newly-formed cusp drops rapidly as the black hole binary transfers energy to the stars.

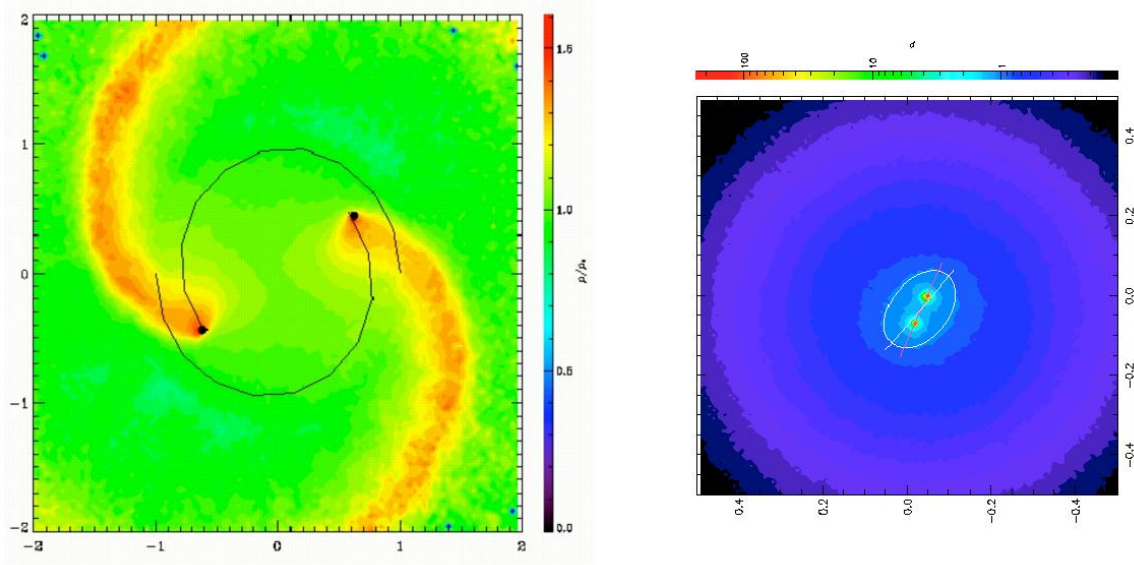


Figure 5: Left panel shows the density perturbation caused by twin black holes orbiting in an isothermal gas clouds (face on view above the orbital plane). Black curves represent the individual orbits of the black holes that spiral in under the action of gas-dynamical friction. In this simulation<sup>124</sup> the mass of the binary is 0.02 of the mass in the gas-sphere. Right panel shows the color-coded density map, in the orbital plane, when the black hole separation  $a < a_{\text{binary}}^{\text{gas}}$ . The two density peaks in red coincide with the location of the black holes. An ellipsoidal deformation with axis misaligned with the respect of the binary axis is present and is exerting a torque on the binary.

holes, initially unbound, excite two prominent density wakes along their mildly transonic orbit and sink toward the center where they form a binary. When the large-scale drag by gas-dynamical friction is no longer effective since  $a$  has decayed below  $a_{\text{binary}}^{\text{gas}}$ , the system develops an ellipsoidal deformation resulting from the superposition of the heads of the wakes. The asymmetry present in the wakes combines to make the ellipsoidal gaseous envelope misaligned with the binary axis, and this is the cause of further decay.

### 3 Black hole dynamics in stellar backgrounds

There are, at present, no simulations of *gas-free* mergers between galaxies with composite structure (i.e. with a dark matter halo, a stellar disk, a bulge and a central black hole) that follow in realism the dynamics of the black holes during phase P  $\rightarrow$  B. Most of the studies start already with a close black hole pair moving inside the gravitational potential of a stellar equilibrium model, and follow in great detail the phase of binary hardening by three-body interactions (phase H), using direct summation codes. These studies have revealed that the rate at which the binary hardens depends sensitively on the properties of the underlying gravitational potential and on the degree of two-body relaxation present in the galaxy's model<sup>103,120,125</sup>.

As the fractional energy exchange per scattering, in three-body encounters, is  $\sim m_*/M_{\text{BH,T}}$ , the rate at which the binary decays is  $-\dot{a}/a \sim (m_*/M_{\text{BH,T}})n_*\sigma A_{\text{BH}} \sim \pi G\rho_*a/\sigma$ , assuming a constant flux of stars ( $\sim n_*\sigma$ ) and a binary cross section  $A_{\text{BH}} \sim \pi a(GM_{\text{BH,T}}/\sigma^2)$  corrected for gravitational focusing. This defines a hardening timescale<sup>120</sup>

$$t_{\text{hard}}^* \sim \frac{\sigma}{\pi G\rho_*a} \sim 7 \times 10^8 \left( \frac{\sigma}{100 \text{ km s}^{-1}} \right) \left( \frac{10^4 \text{ M}_{\odot} \text{ pc}^{-3}}{\rho_*} \right) \left( \frac{10^{-3} \text{ pc}}{a} \right) \text{ yr} \quad (17)$$

which expresses the time it takes the binary to reach the separation  $a$ , from large initial distances, inside a fixed stellar homogeneous background. In galactic nuclei,  $t_{\text{hard}}^*$  determines the initial rate at which the binary hardens. Only stars on near radial orbits with specific angular momentum  $J$  less than  $J_{\text{lc}} \sim (GM_{\text{BH,T}}a)^{1/2}$  experience the field of the individual binary components: this condition defines a selected domain in phase-space, called *loss cone*. As the stellar mass contained in the loss cone of a typical galaxy is less than  $M_{\text{ej}}$ , the black hole orbit decays at a much lower rate once the loss cone is emptied<sup>125</sup>. Whether the black holes can continue to exchange energy and momentum with stars then depends on the efficiency with which stars are re-supplied to the loss cone. The depletion of the orbital population inside the loss cone may thus lead to a *stalling* in the decay rate.

Stars are expected to diffuse across the loss cone boundary through stellar two-body relaxation processes. A small angular momentum perturbation, excited by a star passing by or by the fluctuating component of the gravitational potential, can deflect a star with  $J > J_{\text{lc}}$  into the loss cone  $J < J_{\text{lc}}$ , and this occurs on the two-body relaxation time  $t_{\text{rel}} = t_{\text{cross}}N/(8 \ln N)$  (where  $t_{\text{cross}}$  is the crossing through the galaxy of a typical star). Since  $t_{\text{rel}}$  is often longer than the lifetime of the galaxy's nucleus, stellar dynamical processes are unable to conduct the binary to coalescence, and this theoretical difficulty has been called the *final parsec problem*<sup>120,121</sup>.

This problem has been investigated in depth<sup>101–104,125–132</sup>, and the picture that is emerging goes in the direction of reducing the bridge separating phase H to phase GW, because of the presence of additional mechanisms<sup>125</sup>. In the collisionless background of a massive elliptical where two-body relaxation is unimportant, binary evolution can continue if stars ejected by the black holes remain, after the encounter, inside the loss cone: moving on returning orbits, these stars interact again with the binary for a few times before

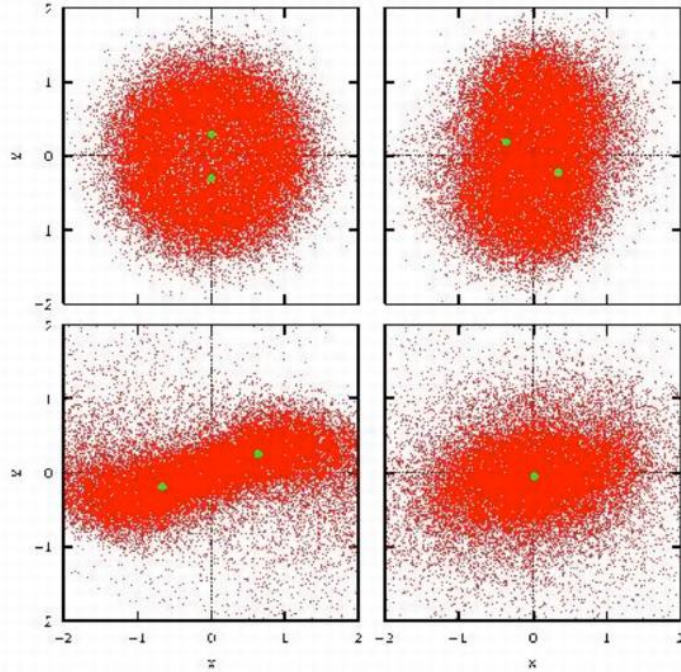


Figure 6: Evolution of a massive black hole binary (of total mass  $M_{\text{BH,T}} = 0.04M_{\text{galaxy}}$ ) in a triaxial, rotating galaxy model<sup>128</sup>. Snapshots show the positions of the 200K particles of the simulation, at four selected times. The twin black holes, indicated in green, initially come together by falling along the bar before forming a bound pair. On a longer timescale the binary hardens at a rate which is found to be independent of the number of particles used, and sufficiently rapid to allow for coalescence in 10 Gyr, even in the absence of collisional loss-cone refilling, providing a potential solution to the final-parsec problem.

they are lost<sup>125</sup>, alleviating the demand on  $M_{\text{ej}}$ . If re-ejection happens to be only marginally important, most relevant is the geometry of the galactic potential. In triaxial nuclei where angular momentum is not a conserved quantity, there exists a potentially larger population of orbits that can encounter the black hole binary<sup>127</sup>. The non-axisymmetric/rotating case in particular allows for the growth of stellar bars<sup>128</sup>. Torques from bar-like potentials then create a population of centro-philic orbits that pass near the center of the galaxy once per crossing time, and that promptly interact with the binary. Figure 6 shows, via a sequence of snapshots, how black holes sink inward along the bar, inside an unstable strongly rotating stellar spheroids<sup>128</sup>. A further mechanism for refilling the loss cone is dynamical relaxation induced by a population of massive perturbers, such as giant molecular clouds or star clusters, that scatter efficiently field stars across the loss cone boundary, leading to rapid coalescence of the binary<sup>130,131</sup>. In galaxies where none of these mechanisms is present and the binary stalls, infall of a "third" massive black hole, during a repeated merger, can accelerate the decay<sup>133,134</sup>. A hierarchical triplet may form, with the third black hole strongly perturbing the hard inner binary through the exchange of energy and angular momentum as in a three-body encounter. If the orbit of the third black hole is inclined relative to the orbital plane of the inner binary, a Kozai resonance lead the eccentricity of the inner binary to such an high value that the two black holes coalesce promptly<sup>135</sup>.

In the dense nuclei of the less massive ellipticals, two-body relaxation may lead to the repopulation of the loss cone. Stars diffuse across the loss cone boundary so that the binary decays on a time  $a/\dot{a} \propto t_{\text{rel}} \propto N$ . This regime is opposite to the collisionless case, and often ellipticals fall in between, having relaxation times comparable to their age. In this case, gravitational encounters contribute to the refilling of the loss cone but the phase-space distribution does not reach steady state. Steep angular momentum gradients at the loss cone boundary are produced after the sudden draining of stars, following the formation of the hard binary. Since the collisional transport rate in phase-space is proportional to these gradients, steep gradients imply an increased flux of stars. This transitory enhancement becomes even most important when the galaxy's nucleus experience repeated mergers or infall. In this case the loss cone returns to an unrelaxed, non-equilibrium state with a large angular momentum gradient<sup>125</sup>.

From the above considerations, refilling of the loss cone either through non-equilibrium relaxation or dynamical relaxation implies a depletion of stars *outside* the loss cone. This process destroys the nuclear stellar cusp producing "missing light". This is at the hart of core scouring by the black hole binary. Since  $M_{\text{ej}}$  gives the stellar mass removed by the binary, and since  $M_{\text{ej}}$  correlates with the binary mass, theory of binary decays finds its most outstanding test in bright ellipticals built from repeated mergers (as mass depletion requires at least  $\mathcal{N}M_{\text{ej}}$  with  $\mathcal{N} \sim 3 - 5$  mergers) where black hole dynamics is dominated by the stellar component of the interacting systems<sup>92,93,120</sup>.

Real binaries likely evolve through a combination of different mechanisms where gas plays also a role. There is a close parallelism between the final parsec problem and the problem of quasar fueling: both requires that a mass in gas and/or star comparable to  $M_{\text{BH,T}}$  or even larger be supplied to the *inner parsec* of the galaxy host within a timescale  $\sim 10^{8-9}$  yr, much shorter than the age of the universe. Observations of powerful AGNs and quasars indicates that Nature accomplishes this probably through inflows triggered by torques from stellar bars<sup>136</sup> and/or unstable, massive gas disks<sup>137</sup>. There is the suspicion that the same inflow of gas that can contribute to the fueling could contribute to the orbital decay of the black hole binary in a number of ways: through viscous torques in self-regulated accretion disks that extract angular momentum from the orbit or through renewed star formation.

## 4 Black hole pairing in gas-rich mergers

The study of black hole dynamics from the state of pairing P down to the GW domain in *gas-rich mergers* is a field in rapid progress. The heavy computational demand and the rich physics involved require to proceed through well defined steps and simplifications in order to have full control of the basic physics and a strategy to attack the complexity which is present when treating with star formation and gas-dynamics. The importance of black hole binary evolution in gaseous background is not only limited to their dynamics. It also involves the physics of accretion that determines the black hole mass growth and spin evolution, and the interaction of the black holes with the environment through their energy and momentum deposition in the interstellar medium<sup>8,10</sup>. These processes are inter-related and touch many aspect of galaxy and AGN evolution. In describing the first key results, it will become clear that the body of data from simulations is still inhomogeneous, and many question remain unanswered. While black hole dynamics in collisionless systems has been explored mainly in the hardening phase H where the numerical challenge is the highest, black hole dynamics in dissipative/collisional systems has been mainly studied from the onset of pairing, in gas-rich galaxies simulated with some realism, down to the onset of the hardening phase H that occurs, when/if present, inside a massive nuclear disk, immersed in a massive bulge. Trial runs with galaxies either gas-free or with a hot-virialized gas component, have been carried out to test the sensitive dependence of black hole pairing<sup>138</sup> on the background models. These trials reveal that we are still far from having a unified view of the fate of black holes, and in the incoming paragraphs we will summarize key findings and open problems.

### 4.1 Rapid birth of a black hole binary in the aftermath of a major merger

Galaxies, as observed in our low-redshift universe, are multi-component systems of collisionless dark matter and stars that coexist in equilibrium with either a hot or cold multi-phase gaseous component: a central massive black hole is also part of this landscape. Simulating a collision between two galaxies thus requires the versatile tool of hydrodynamical simulations.

The merger of two spiral galaxies similar to the Milky Way represents the prototype of a galaxy collision, and it has been studied in the literature typically with force resolution of  $\gtrsim 100$  pc<sup>11,112,138–140</sup>. The merger of two spirals with black holes complements these studies, representing a real numerical challenge as in the simulation there is the need to reach/maintain a force resolution on a scale as small as 5 – 10 pc in order to accurately trace the hole’s dynamics down to  $a_{\text{binary}}^{\text{gas,star}}$ . This is the ”minimal” request that can be attained with gradual resizing of the computational volume via splitting techniques.

Figure 7 shows the outcome of a merger, selected among a suite of simulations with different encounter geometries and disk orientations by Mayer et al.<sup>141</sup>. Here, twin Milky Way like galaxies approach each other on a parabolic prograde coplanar orbit with pericentric distance equal to 0.2 of the galaxy’s virial radius, typical of cosmological mergers. Each galaxy model comprises a central black hole of  $3 \times 10^6 M_{\odot}$  lying on the observed  $M_{\text{BH}}$  versus  $\sigma$  relation, a stellar bulge (modeled as an Hernquist sphere of mass  $M_{\text{Bulge}} = 0.008M_{\text{vir}}$ ), an exponential disk of stars and gas (with total mass  $M_{\text{disk}} = 0.04M_{\text{vir}}$  and gas fraction  $f_{\text{gas}} = 10\%$ ), and a massive ( $M_{\text{vir}} = 10^{12} M_{\odot}$ ) extended dark matter halo with NFW density profile<sup>142</sup>. Simulations are performed using the N-Body/SPH code GASOLINE<sup>143</sup>. Gas thermo-dynamics includes a recipe of star formation and radiative cooling down to a relatively high floor temperature of 20,000 K to account for turbulent heating, non-thermal pressure forces and the presence of a warm interstellar medium.

The galaxies first experience a few close fly-by (upper six panels of Figure 7) during which tidal forces start to tear the galactic disks apart, generating tidal tails and plumes. The steep potentials at the center of both

galaxies allow the survival of their baryonic cusps that sink under the action of dynamical friction against the dark matter background, dragging together the two black holes. During the last close passage, prior merger, strong spiral patterns appear in both the stellar and gaseous disks: non axisymmetric torques redistribute angular momentum so that as much as 60% of the gas originally present in each disk of the parent galaxy is funneled inside the inner few hundred parsecs of the individual galaxy cores. This is illustrated in the middle panel of the last row. The black holes, still in the pairing phase P, are found to be surrounded by a rotating stellar and gaseous disk of mass  $\sim 4 \times 10^8 M_\odot$  and size of a few hundred parsecs. The two black holes with their own disks are just 6 kpc far apart and accretion (not resolved on this scale) is expected to light up the two black holes as in the case of NGC 6240. In the meantime a star-burst of  $30 M_\odot \text{ yr}^{-1}$  has invested the central region of the on-going merger. It is worth noting that already at this stage the dissipative role of gas changes the black hole environment. While in the collisionless case (as depicted in Figure 4) the black holes pair inside their stellar cusps that preserve their density, in the dissipative case they pair inside a denser background resulting from gas-dynamical instabilities that have funneled additional mass in the hole’s surroundings.

At this stage of the simulation, a computational volume of 30 kpc in size is refined in order to achieve a force resolution of 2 pc and continue the study of the black hole’s dynamics. The fine-grained region selected is large enough to guarantee that stars and dark matter particles essentially provide a smooth background, while the computation focuses on the gas component which dominates by mass in the region. The short dynamical timescale involved in this phase (1 – 10 Myr) compared to the star-burst duration ( $\sim 100$  Myr) suggests to model the thermodynamics and radiation physics simply via an effective equation of state. Calculations that include radiative transfer show that the thermodynamic state of a metal rich gas heated by a star-burst, comprising stellar feed-back, can be approximated by an equation of state of the form  $P = (\gamma - 1)\rho u$  with  $\gamma = 7/5$  where the specific internal energy  $u$  evolves with time as a result of  $PdV$  work and shock heating<sup>144,145</sup>.

With time, the two baryonic disks eventually merge in a *single massive self-gravitating, rotationally supported nuclear disc* of  $\lesssim 100$  pc in size, now weighing  $3 \times 10^9 M_\odot$ . This *grand disk* is more massive than the sum of the two nuclear disks formed earlier because radial gas inflows occur in the last stage of the galaxy collision. A strong spiral pattern in the disk produces remarkable radial velocities whose amplitude declines as the spiral arms weaken over time. Just after the merger, radial motions reach amplitudes of  $\sim 100 \text{ km s}^{-1}$ , and possibly feed the black holes on flight. The nuclear disk is surrounded by a more diffuse, rotationally-supported envelope extending out to more than a  $\sim$  kpc from the center and by a background of dark matter and stars distributed in a spheroid. This grand disk is rotationally supported ( $v_{\text{rot}} \sim 300 \text{ km s}^{-1}$ ) and also highly turbulent, having a typical velocity  $v_{\text{turb}} \sim 100 \text{ km s}^{-1}$ . Multiple shocks generated as the galaxy cores merge are the main source of this turbulence. The disk is composed by a very dense, compact region of size about 25 pc which contains half of its mass (the mean density inside this region is  $> 10^5 \text{ atoms cm}^{-3}$ ). The outer region instead, from 25 to 75-80 pc, has a density 10-100 times lower. The disk scale height also increases from inside out, ranging from 20 pc to nearly 40 pc. The volume-weighted density within 100 pc is in the range  $10^3 - 10^4 \text{ atoms cm}^{-3}$  compatible to the observed nuclear disks<sup>146-149</sup>. This suggests that the degree of dissipation implied by the effective equation of state gives a reasonable description of reality despite the simplicity of the thermodynamical scheme adopted.

After 5.12 Gyr from the onset of the collision, the black holes, dragged toward the dynamical center of the merger remnant, move inside the grand disk spiraling inward under the action of gas-dynamical friction. In less than  $\lesssim 1$  Myr, a timescale much shorter than the duration of the star-burst, the relative black hole orbit

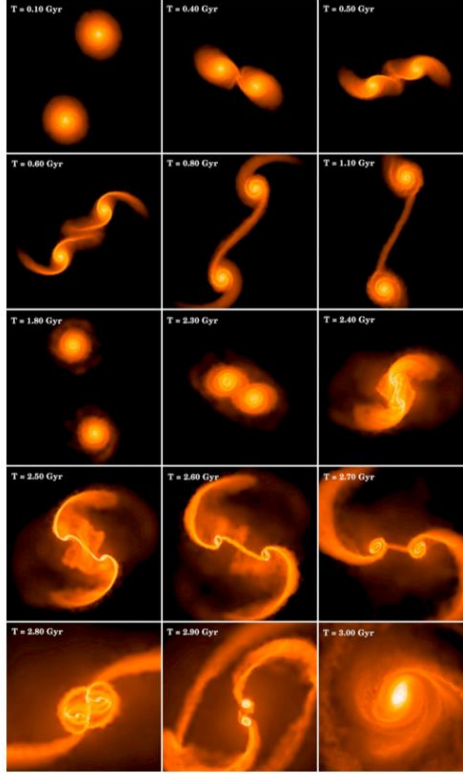


Figure 7: A major merger between two Milky Way like galaxies<sup>141</sup>: the simulation follows the evolution of dark matter, stars, gas, and of the massive black holes ( $M_{\text{BH}} = 3 \times 10^{-3} M_{\text{Bulge}}$ ), but only the gas component is visualized for seek of clarity. Brighter colors indicate regions of higher gas density and the time corresponding to each snapshot is given by the labels. The first 10 images measure 100 kpc on a side, roughly five times the diameter of the visible part of the Milky Way galaxy. The next five panels represent successive zooms on the central region. The final frame shows the inner 300 pc of the nuclear region at the end of the simulation.



decay from  $\sim 100$  pc to  $\lesssim 5$  pc where they form a *binary*, as mass of gas enclosed within their separation is less than the mass of the binary. It is the gas that controls the orbital decay, not the stars. The transition between state P to B is now completed as illustrated in Figure 8: a mildly eccentric binary ( $e \sim 0.5$ ) has formed with orbital period of  $10^5$  yr. This short sinking timescale comes from the combination of two facts: that gas densities are higher than stellar densities in the center due to the dissipative nature of the interaction, and that the black holes move relative to the background with mildly supersonic velocities where the drag is the highest<sup>141</sup>. But, how sensitive are the results on the input physics?

Mayer et al.<sup>141</sup> have decreased the degree of dissipation by increasing  $\gamma$  to  $5/3$ , to mimic the presence of a heat source. It is found that in this warmer environment, a turbulent, pressure supported cloud of a few hundred parsecs forms rather than a rotationally supported cold disk. The mass of gas is lower within 100 pc relative to the  $\gamma = 7/5$  case because of adiabatic expansion following the final shocks, at the time of merging of the two cores. The nuclear region is still gas dominated, but the stars/gas ratio is  $> 0.5$  in the inner 100 pc. The black holes in this hotter environment follow a "retarded" dynamics: the transit from P  $\rightarrow$  B is not any longer seen, over a time span of  $\lesssim 1$  Myr. The black holes remain at a distance of 50-150 pc, as shown in Figure 8, and a bound system is expected to form, according to eq. 9, on a time scale  $t_{\text{DF}} \sim 10^7$  yr, under the joint control of stars and of the lower density gas.

The radiative injection of energy from the black holes accreting on flight might be a candidate for a heating source, and for increasing the turbulence in the gas by injecting kinetic energy<sup>150,151</sup> in the surrounding medium, possibly creating outflows. A rough estimate for the energy released in the accretion process is  $\Delta E_{\text{acc}} \sim f_{\text{dep}}(L/L_E)(t/t_{\text{Ed}})\epsilon M_{\text{BH}}c^2$  (with  $L_E$  the Eddington luminosity,  $\epsilon \sim 0.1$ , and  $f_{\text{dep}}$  the fractional energy deposited by the accreting black hole in the surrounding gas). This energy is  $\Delta E_{\text{acc}} \sim 2 \times 10^{57}$  erg, for a black hole mass of  $10^6 M_{\odot}$  accreting at the Eddington limit for a time  $t_{\text{Ed}} \sim 10^7$  yr, and  $f_{\text{dep}} = 0.01$ . This energy appears to be larger than the energy dissipated by the binary in its inspiral down to  $a_{\text{GW}}$ ,  $\Delta E_{\text{B}} = GM_{\text{BH,T}}\mu_{\text{BH}}/2a_{\text{GW}} \sim 6 \times 10^{54}$  erg. Energy released on flight by the black holes can influence the thermal state of the grand disk which is supposed to convert a sizable fraction of its gas into stars. This environmental change is expected to affect the dynamics and the fueling of black holes (even after black hole coalescence) with consequences that have not been exploited yet, given the computational challenge that these processes pose.

Increasing the resolution will be the next priority. At higher spatial resolutions ( $\gtrsim 10^{-3}$  pc), the grand disk is expected to reveal a much richer structure with spiral patterns and bars, considered as possible candidates for triggering small scale inflows around the black holes. Regions that appear featureless in low resolution runs should instead reveal the true nature of the gas. Wada & Norman<sup>152</sup> showed that when the main radiative processes and the feedback from supernovae are directly incorporated in simulations of rotating gaseous disks, a multi-phase turbulent interstellar medium arises naturally due to the interplay between gravitational/thermal instabilities and energy injection by supernovae. The resulting structure is clumpy at all scales. This is a clear example that there is still some *missing* physics that needs to be incorporated, beyond polytropes.

## 4.2 Pairing in minor mergers

Pairing seems inescapable in major, equal-mass mergers: the violence of the collision affecting both galaxies in a nearly symmetric fashion (regardless the geometry of the encounter) brings the two black holes in the central region of the remnant. There, in presence of a cold nuclear disk, a binary forms rapidly within a Myr

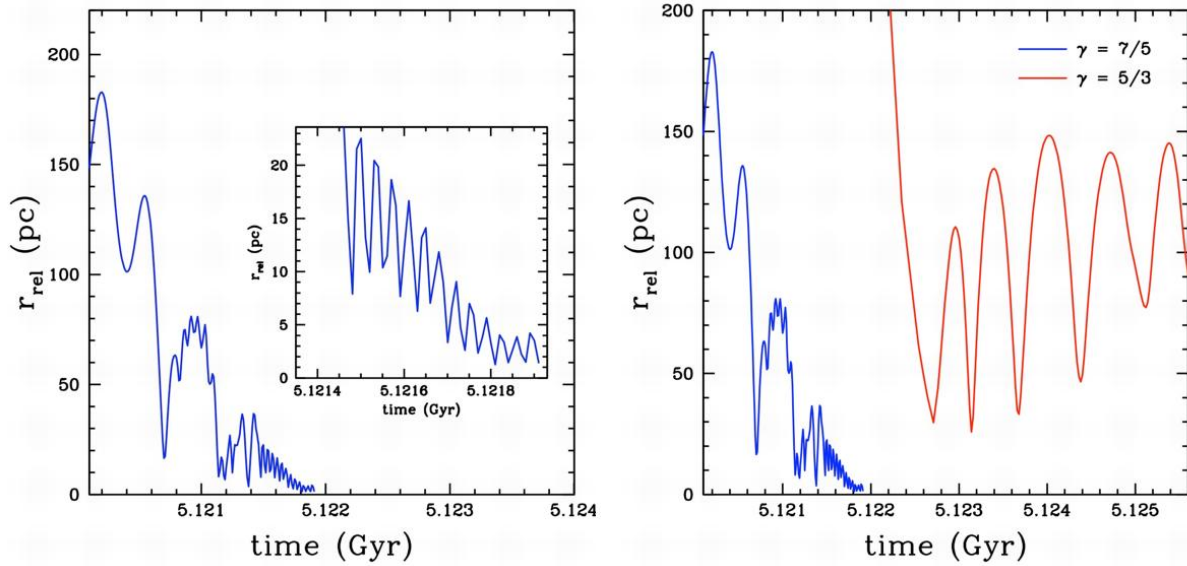


Figure 8: Orbital separation of the two black holes as a function of time during the last stage of a selected galaxy merger when a massive nuclear disk forms<sup>141</sup>. The orbit of the pair is eccentric until the end of the simulation. The two peaks at scales of tens of parsecs mark the end of the phase during which the two holes are still embedded in two distinct gaseous cores. Until this point the orbit is the result of the relative motion of the cores combined with the relative motion of each black hole relative to the surrounding core, explaining the presence of more than one orbital frequency. The inset shows the details of the last part of the orbital evolution which takes place in the nuclear disc arising from the merger of the two cores. The binary stops shrinking when the separation approaches the softening length (2 pc). In the right panel, the blue line shows the relative black hole distance as a function of time for the run with  $\gamma = 7/5$  as shown in the left panel, while the red line shows it for  $\gamma = 5/3$ .

after the merger is completed. But, what about pairing in minor merger? Minor, i.e. unequal-mass mergers differ profoundly from major mergers. Encounters are uneven, resembling more an "accretion" process than a merger as the less massive galaxy is dramatically damaged during its sinking into the primary by tidal and ram pressure forces.

Simulations by Boylan-Kolchin<sup>153–155</sup> of collisionless spherical halos shows how details on the encounter geometry, satellite-to-host mass ratio, internal structure (dark matter plus bulge), and on presence (absence) of a central black hole in the main host affect the degree of damage of the satellite resulting in a broad variety of outcomes. Satellites on less-bound, eccentric orbits are more easily destroyed than those on more-bound or more-circular orbits as a result of an increased number of pericentric passages and greater cumulative effects of gravitational shocking and tidal stripping. In addition, satellites with densities typical of faint elliptical galaxies are disrupted relatively easily, while denser satellites can survive much better in the tidal field of the host. Also satellites merging on to a host with a central black hole are more strongly disrupted than those merging on to hosts without the black hole. Thus, it is not surprising that also black hole pairing is affected in major ways by these details. It is clear that investigating the necessary conditions for pair formation in minor mergers with gas is of primary importance, both in a broad cosmological context, and for the impact on the *LISA* data stream.

Callegari et al.<sup>156</sup> find different outcomes, in their systematic study of 4:1 (i.e. mass ratio  $q = 0.25$ ) and 10:1 (i.e.  $q = 0.1$ ) collisionless and gas-dynamical mergers, performed with GASOLINE at various cosmic epochs. Specifically, the 4:1 mergers are studied in the local Universe ( $z = 0$ ), while the 10:1 mergers at  $z = 3$ , assuming a constant  $M_{\text{BH}} - M_{\text{Bulge}}$  relation in between these cosmic epochs<sup>4</sup>, and rescaled models, replica of the Milky Way, for the galaxies. In the  $z = 3$  runs, the black hole masses are thus  $6 \times 10^5$  and  $6 \times 10^4 M_{\odot}$ , so that their expected inspiral and coalescence signal falls nicely in the *LISA* sensitivity window<sup>29,30</sup>.

All collisionless cases, regardless the value of  $q$ , do not lead to the formation of a close black hole pair: tidal shocks progressively lower the density in the satellite until it dissolves, leaving a wandering black hole in the remnant. Only with the inclusion of a gaseous disk component, inclusive of radiative cooling, star formation, and supernova feedback, the merger changes significantly. Figure 9 depicts the star-forming gaseous component of the satellite, to show its profound structural damage (the primary is not shown). For mass ratios 4:1 at  $z = 0$ , bar instabilities excited at pericentric passages funnel gas (present in a fraction  $f_{\text{gas}} = 0.1$  of the total disk mass) to the center of the satellite, steepening its potential well and allowing its survival against tidal disruption down to the center of the merger remnant. Therefore in this case, the presence of a dissipative component is necessary and sufficient to pair the black holes down to the force resolution limit of  $\sim 100$  pc scales, and to create conditions favorable to the formation of a binary. Instead, the smaller satellites (in the 10:1 mergers at  $z = 3$ ) are more strongly affected by both internal star formation and the gas-dynamical interaction between their interstellar medium and that of the primary galaxy. Torques in the early stages of the merger are not acting to concentrate gas to the center, due to the absence of a stellar bar and the stabilizing effect of turbulence. As a result, ram pressure strips all of the interstellar medium of the satellite. Still, gas-rich satellites (with  $f_{\text{gas}} = 0.3\%$ ) undergo a central burst of star formation during the first orbits which increases their central stellar density, thus allowing their survival and ensuring the pairing of the two black holes via dynamical friction in a few  $10^8$  yr after the disruption of the satellite. By contrast, in a satellite with lower gas content ( $f_{\text{gas}} = 0.1\%$ ) star formation is not effective in enhancing its concentration: as a consequence, even its central region is disrupted at a few hundred parsecs from the center of the primary, and the pairing between the two black holes is delayed by a few billion years. The sensitive dependence of pairing in minor mergers suggests that there exist a *minimum* mass ratio for the

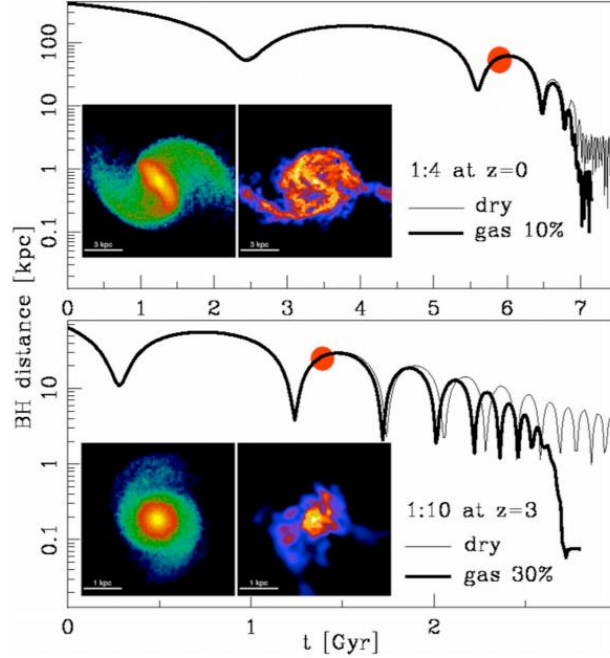


Figure 9: Black hole relative separation as a function of time in four simulations<sup>156</sup>. In the upper row, the hole’s distance refers to two selected 4:1 mergers (for galaxy models at  $z = 0$ ); the thin and thick lines correspond to simulations with no-gas (dry) and with gas ( $f_{\text{gas}} = 0.1\%$ ), respectively. In the lower row, the hole’s distance refers to 10:1 mergers (for galaxy models at  $z = 3$ ); the thin and thick lines correspond to simulations with no-gas (dry) and with gas ( $f_{\text{gas}} = 0.3\%$ ), respectively. The insets show the color-coded density maps of stars (left) and gas (right), on a box of 4 kpc on a side. The large dot on each curve indicates the time at which the two snapshots are recorded. Colors code the range  $10^{-2} - 1 M_{\odot} \text{pc}^{-3}$  for stars, and  $10^{-3} - 0^{-1} M_{\odot} \text{pc}^{-3}$  for the gas. These snapshots are representative of the average behavior of the satellites during the first two orbits. Note the formation of a strong bar for the 4:1 minor merger, which is absent for the 10:1 case, and the truncation of the gaseous disk in the 10:1 satellite caused by ram pressure stripping.

interacting galaxies below which phase B is unattended. These simulations<sup>156</sup> suggest that a 10:1 merger is nearing this limit, depending sensitively on the fraction of gas present in both galaxies.

## 5 Black hole dynamics in self-gravitating nuclear disks

As shown in Section 4.1, major mergers between multi-component galaxies lead to the pairing of black holes inside the turbulent, gaseous disk that forms in the aftermath of the collision. Ideally, a large set of simulations should be carried on to explore how black holes transit from P→B→H, under a variety of initial conditions. To encompass the enormous computational effort, a number of authors explored (using GADGET) black hole sinking in a two-component system, i.e. an equilibrium circum-nuclear disk embedded in a stellar bulge<sup>157–131</sup>, viewed as relics of the merger. In all these studies, the equilibrium disk is modeled as a self-gravitating Mestel disk of size ( $R_0 \lesssim 100$  pc), mass ( $M_{\text{disk}} = 10^8 M_{\odot}$ ) and vertical scale height ( $H \sim 10$  pc), as close as indicated by observations of massive nuclear disks in Seyfert and ULIRGs<sup>117–120</sup>. Stars follow a Plummer profile and their mass within the spherical volume of radius  $R_0$  is five times the disk mass, as suggested by observations<sup>146</sup>.

In modeling the gas disk, thermodynamics plays a critical role. In real astrophysical disks, massive gas clouds coexist with warmer phases and a simple isothermal equation of state would provide an unrealistic averaged representation of the real thermodynamical state. Cold self-gravitating disks are unstable to fragmentation and find their stability as soon as stars, resulting from the collapse and/or collision of clouds, inject energy in the form of winds and supernova blast waves, feeding back energy into the disk now composed of stars and a multiphase gas. Due to the complexity of implementing in a code this rich physics at the required level of accuracy, a simple polytropic equation of state of the form  $P = K\rho^\gamma$  is introduced to capture the basic thermodynamical behavior of the gas.  $K$  is a free parameter corresponding to the entropy of the gas and  $\gamma$ , varying between 1 and 5/3, is a parameter that can be tuned to represent either a pure adiabatic response ( $\gamma = 5/3$ ) or a response that mimics cooling, star formation and feedback ( $\gamma = 7/5$ ) as in Mayer et al.<sup>141</sup>.

Escala et al.<sup>128</sup> consider cases where  $K$  varies to reproduce different degrees of clumpiness, keeping  $\gamma$  fixed to 5/3, while Dotti et al.<sup>131</sup> explore, in a complementary fashion, cases with  $\gamma = 5/3$  and 7/5, and fixed  $K$ . Escala et al.<sup>157</sup> assume equal mass black holes moving on circular orbits, varying the black hole mass to disk ratio, and the angle between the orbital plane of the pair and the circum-nuclear disk. Dotti et al.<sup>158–160</sup> explore the dynamics of both equal and unequal mass black holes starting from eccentric, prograde or retrograde orbits that may arise from arbitrary encounter geometries and minor merger events.

The main results of all these works can be summarized as follows: (i) the black holes always reach separations of a few parsecs in  $\lesssim 10$  Myr, and form a Keplerian binary; (ii) the pairing process is faster in colder disks and for black holes orbiting in the disk plane; (iii) black holes on initially eccentric prograde orbits lose memory of their initial eccentricity and form binaries consistent with  $e \sim 0$ ; (iv) retrograde eccentric orbits turn into prograde near-circular orbits before the black holes form a bound system; (v) very massive binaries perturb the disk globally and excavate transitory gaps in the circum-binary environment.

### 5.1 Black hole inspiral, circularization and orbital angular momentum flip

In the rotating background of a Mestel disk, the black holes on circular orbits excite prominent wakes both in front of and behind their path, but the wake that forms behind is the most effective in exchanging angular

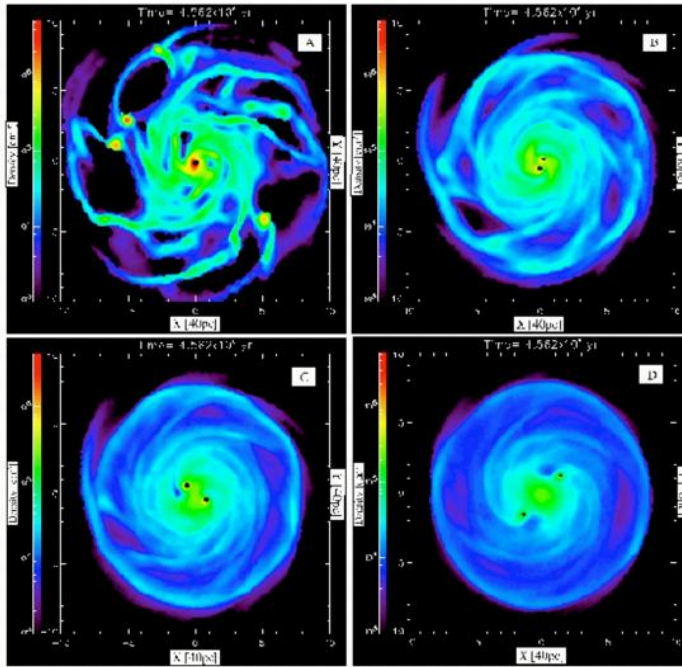


Figure 10: Face on view of the density distribution of a gaseous Mestel disk hosting two equal mass black holes<sup>157</sup> (with  $M_{\text{BH}} = 0.01M_{\text{disk}}$ ). The black dots indicate their position, recorded at the same time. The disk clumpiness varies according to the parameter  $K$ . The form of the density distribution is smooth for large values of  $K$  (run D) and shows spiral waves, while it is highly inhomogeneous for small  $K$ , as dense clumps and filaments form as a result of a lower pressure support against gravitational pull.

momentum given the rotation pattern and surface density profile of the disk<sup>158</sup>. This causes a net braking and the black holes end forming a binary in less than 10 Myr.

Braking by gas-dynamical friction depends also on the level of disk clumpiness that introduces a noise element on the black hole dynamics: clumps perturb the black hole orbits more strongly and at random phases so that their inspiral is more rapid and chaotic. In smoother background the perturbation instead takes the form of a spiral wave. Figure 10 depicts snapshots of the face-on density distribution of the gas disk and current black hole position, obtained for four different runs with increasing  $K$ , and computed at the same time, from Escala et al. <sup>157</sup>. In the cold clumpy disk, black holes have decreased their separation by more than a factor 10 reaching, the numerical resolution length. The sensitivity to clumpiness suggests a parallelism with stellar systems: as large clumps (likely in the form of dense molecular clouds) accelerate binary hardening in gaseous disks, the same holds true in stellar backgrounds where molecular clouds accelerate loss cone refilling and so black hole inspiral.

Circularization in a smooth (high  $K$ ) rotating disk is also a clear prediction of these studies<sup>159</sup>. When the black holes move on eccentric orbits, circularization takes place well before the black holes form a binary and this is a feature peculiar to dynamical friction in a rotating background. On an initially eccentric orbit, the black hole has, near periapsis, a velocity larger than the local rotational velocity, so that dynamical friction causes a reduction of its velocity: the wake of fluid particles lags behind the black hole trail. By contrast, near apoapsis, the black hole velocity is lower than the disk rotational velocity, and in this case, the wake is dragged *in front* of the black hole’s trail, causing a positive tangential acceleration. The composite effect is a decrease of  $e \rightarrow 0$ . In spherical backgrounds, dynamical friction tends to increase/maintain the eccentricity, both in collisionless<sup>116,161,162</sup> and in gaseous<sup>163</sup> environments. This is suggestive that the presence of a rotating gaseous background can be inferred from the smallness of the binary eccentricity on scales of a few parsecs.

A further recently discovered signature of a rotating background is the angular momentum flip of initially counter-rotating orbits<sup>160</sup>. This has been highlighted when considering the inspiral of a black hole (called secondary) moving in a Mestel disk with  $\gamma = 7/5$  and hosting at the center a primary black hole. The initially negative angular momentum of the moving black hole grows very fast during the first million year. The black hole-disk interaction brakes the hole at all orbital phases, because the hole’s velocity and disk flow pattern are anti-aligned and the density wake lags away behind the hole. The increase of the orbital angular momentum is further facilitated by the fact that, while the orbit decays, the black hole interacts with progressively denser regions of the disk. The orbit is nearly radial at the time the orbital angular momentum changes sign and this occurs before the secondary binds to the central black hole. When co-rotation establishes, the orbital momentum increases under the circularizing action of dynamical friction in its co-rotating mode. This orbital *flip* has been visible thanks to the high numerical resolution adopted (0.1 pc through the entire simulation) that allows to trace the gas-black hole interaction with unprecedented accuracy. In conclusion, a further prediction of black hole inspiral in rotating disks is that gas-dynamical friction conspires to drive counter-rotating orbits in co-rotation before the time of formation of a Keplerian binary.

## 5.2 Accretion on flight

Accretion can be studied only if the resolution length-scale of the code is smaller than the Bondi-Hoyle-Littleton radius of the moving black hole. If this resolution is achieved, as in a recent series of simulations<sup>160</sup>,

its is possible to follow the fueling of the black hole *on flight*, i.e along its motion, and also to include the contribution of the drag force  $\mathbf{F}_{\text{BHL}}^{\text{gas}}$  due to accretion from the numerical self-consistent measure of  $\dot{M}$ . While in previous studies, each black hole was treated as a collisionless particle, now the hole is a *sinking* particle, ready to capture gas within  $R_{\text{BHL}}$  while orbiting inside the disk.

In a recent study<sup>160</sup>, accretion onto the secondary, moving black hole has been traced starting either from a prograde or a retrograde eccentric orbit relative to the disk’s rotation. It is found that as long as the orbit of the moving black hole remains eccentric, accretion occurs at a low rate, with an Eddington factor  $f_{\text{Ed}}$  (defined as the mass accretion rate  $\dot{M}$  in units of the Eddington rate) close to 0.1, due to the large relative velocity between the black hole and the fluid, and is highly variable owing to the presence of inhomogeneities in the gas in the vicinity  $R_{\text{BHL}}$ . Only when the orbit has circularized (and flipped for the retrograde case), the moving black hole accretes at high rate with  $f_{\text{Ed}} \sim 0.9$  and in a less variable fashion. Thus, two accretion phases are present for the moving black hole: the first is the low/variable state that occurs before circularization (and/or angular momentum flip) and the second is the high/constant state after circularization in the co-rotating mode. By contrast, the central black hole undergoes accretion at an almost constant rate  $f_{\text{Ed}} \sim 0.9$ , in the absence of a substantial motion.

What is the fate of gas inside the black hole sphere of influence  $R_{\text{BHL}}$ ? In the simulations, it is possible to keep record of the specific energy and angular momentum of every accreted fluid particle as a function of time. As the gas density in the black hole vicinity (near  $R_{\text{BHL}}$ ) can be as high as  $10^7 \text{ cm}^{-3}$ , it is conceivable that dissipative/radiative processes operate to reduce the gas internal energy below the values adopted in the simulations. In these circumstances, we expect that the fluid particles bound to each black hole form a geometrically thin, accretion disk in Keplerian rotation. Since every gas particles is found to carry a net angular momentum in the direction parallel to that of the grand nuclear disk, the size of the coplanar accretion disk can be computed according to angular momentum conservation:  $R_{\text{BH,disk}} \sim L_{\text{ver}}^2 / (G M_{\text{BH}})$ , where  $L_{\text{ver}}$  is the vertical component of the specific angular momentum of the particles bound, relative to each hole. After circularization,  $R_{\text{BH,disk}}$  can be as small as 0.01 pc for the very bound particles, strongly suggesting that both black holes are fed through a thin, cold accretion disk along the course of the inspiral<sup>159</sup>. Viscosity (of magneto-rotational origin) is expected to self-regulate the transport of angular momentum in the small Keplerian disks, so that gas flows onto each black hole at the rate determined by the physical conditions of the gas at the outer boundary.

### 5.3 Hardening in a gaseous environment: binary stalling on sub-parsec scales?

With increased *spatial* and *mass* numerical resolution, binary hardening has now being explored down to separations close to  $R_{\text{BHL}}$ . Figure 11 illustrates the outcome of the high resolution simulation by Dotti et al. describing the hardening process through phases P  $\rightarrow$  B  $\rightarrow$  H, for a prograde and retrograde initially eccentric orbit. Orbital decay, guided by gas-dynamical friction, continues from the  $\sim 10$  pc scale down to  $\sim 0.5$  pc, maintaining the same derivative across this domain. When the black hole separation is  $\lesssim 0.5$  pc the derivative steepens indicating that the nature of the black hole-disk interaction has changed. As first indicated by Escala et al.<sup>124</sup>, torques resulting from the ellipsoidal deformation, arising from the superposition of the interacting wakes, accelerates the orbital decay. Only when the black hole separation reaches the resolution limits of the gravitational and hydrodynamical forces the binary stalls, as artifact of the numerical resolution. The rapid decay is a feature present in the  $\gamma = 7/5$  runs, i.e. when the thermodynamical treatment allows from



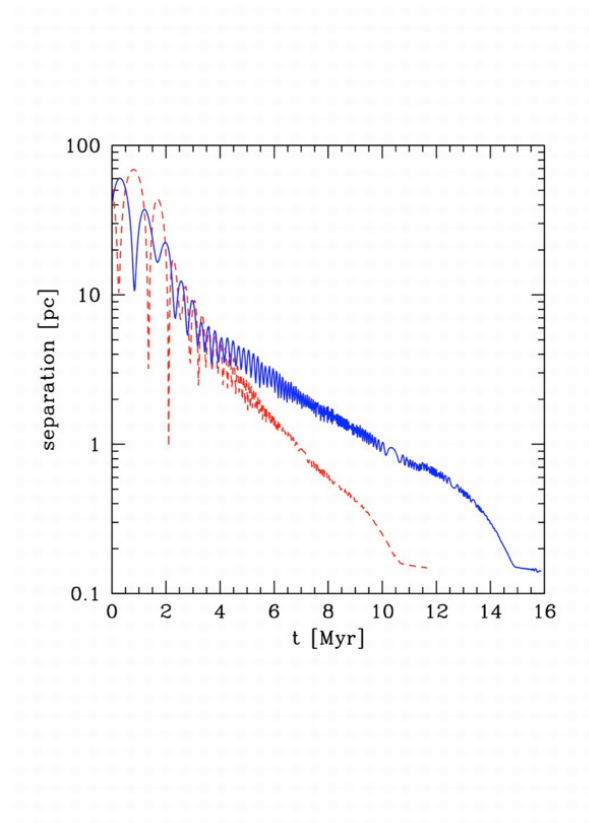


Figure 11: Black hole relative separation as a function of time, as inferred from two high resolution simulations by Dotti et al. (in preparation). Blue-solid (red-dashed) line refers to the case where the moving black hole is set initially on a co-rotating (counter-rotating) orbit with  $e = 0.7$ . In the gaseous background of the rotating Mestel disk (with  $\gamma = 7/5$ ) the binary decays transiting across the three phases, from pairing P, to B where a Keplerian binary forms, down to the hardening phase H.

some degree of dissipation. Equivalent runs for  $\gamma = 5/3$  show evidence of stalling suggesting that dissipative processes play a critical role in determining the black hole dynamics and fate below  $\sim 1$  pc.

Reaching the scale  $a_{\text{GW}}$  is still a numerical challenge because not only it requires an increasingly high resolution, but new input physics. The physics that is described in the next section will rely on the assumption that the gaseous nuclear disk remains on all scales gaseous, i.e. immune by episodes of star formation and feed-back, and that in the near vicinity of the black hole binary the gas has cooled down to form a *circum-binary* disk. The black holes themselves carry their own small, tidally truncated accretion disks (confined within their Roche lobes). These disks can be either consumed or replenished, but their presence will be ignored in the next Section as they play a marginal role in the hole's dynamics. Only in Section 6, these disks will be considered as they play a major role in determining the electro-magnetic signature of binary black holes during their inspiral down to coalescence, and after their merger.

## 5.4 Circum-binary discs and black hole migration

Consider the case of two equal-mass black holes surrounded by a circum-binary disk. What is the physical state of this disk? At the radii of greatest interest, typically of 0.1 pc, the circum-binary disk is expected to be *self-gravitating* as it likely carries a mass  $M_{\text{CBD}}$  in excess of  $\sim 0.1M_{\text{BH,T}}$ : self-gravity controls the gas dynamics so that the circum-binary disk differs from a canonical, geometrically thin accretion disk<sup>164</sup>. In this *hybrid* configuration, the rotation curve is not fully Keplerian (with  $\Omega_{\text{K}} = (GM_{\text{BH,T}}/R^3)^{1/2}$ ), the surface mass-density  $\Sigma(R)$  still declines as in a Mestel disk ( $\Sigma \propto R^{-1}$ ), and the vertical scale height, which for a Keplerian disk is  $H_{\text{K}} \sim c_{\text{s}}/\Omega_{\text{K}}$ , takes instead the expression  $H \sim c_{\text{s}}^2/\pi G\Sigma$ .

The stability of self-gravitating accretion disks around *single* black holes has been investigated extensively in recent years<sup>165–169</sup>. In these disks, large scale disturbances excited by self-gravity cannot always be stabilized nor by pressure gradients (at short wavelengths) nor by rotation (at longer wavelengths). When the non-linear outcome of the instability is particularly violent, fragmentation of the disk into gravitationally bound clumps occurs, turning gas into stars. But there are regimes of interest here, where self-gravity affects the disk structure by exciting non-axisymmetric instabilities that redistribute the angular momentum across the disk without major damage. Crudely, the dividing line from these two different behaviors is set by the Toomre parameter  $Q = c_{\text{s}}\Omega/\pi G\Sigma$ , varying with distance  $R$  across the disk: disks are unstable to fragmentation in regions where  $Q < 1$ ; those with higher sound or turbulence speeds and lower surface densities tend instead to be stable and have  $Q \gtrsim 1$  at all radii.

Astrophysical disks may form initially with  $Q \gtrsim 3$ , but radiative losses are expected to cool the disks down, until eventually  $Q \lesssim 1$ . Numerical simulations show that at this stage, any perturbed disk develops a gravitational instability in the form of a spiral pattern. Compression and shocks induced by the instability lead to a net energy redistribution/deposition and the disk heats up. The instability thus self-regulates its growth in a way that the disk is kept close to marginal stability. Thus astrophysical disks are expected to evolve into a quasi-stable stationary state down to  $Q \sim 1$ , and to sustain an *accretion* flow with outward angular momentum transport through spiral waves<sup>169</sup>.

Circum-binary disks around massive black hole binaries are poorly known theoretically. We do not know how they are fed from the outer massive nuclear disk present on the  $\sim 100$  pc scale, and how they evolve. When a black hole binary is at the center of a self-regulated disk, its time-varying gravitational field is expected to perturb the disk, and in particular its inner rim. The binary, acting as a source of angular momentum,

exerts a tidal torque that inhibits the gas from drifting inside its orbit. This creates a hollow density region, called *gap*<sup>170–174</sup>, that surrounds the binary. Further interaction between the binary and the disk depends on the way the excess of orbital angular momentum of the binary, transmitted to the disk, is redistributed through viscous torques and/or spiral patterns in the fluid, on the way the disk is fed and on its stability against fragmentation.

Gap formation can be understood, in these disks, using dynamical friction as key concept. Consider, for simplicity, the only presence of an inviscid ring of gas skimming the black holes on a circular orbit at a radius  $R$  slightly larger than the binary separation  $a$  ( $R \gtrsim a$ ), and focus on the fate of a fluid parcel. As the fluid parcel moves more slowly than the black holes, it is exerting a drag that tends to decelerate the black holes. The fluid element, accelerated tangentially by the gravitational pull of the black hole closest to it, reacts drifting back with an excess of orbital angular momentum. As a result the entire ring will eventually drift away increasing its distance from the binary: the annular region that was filling the space near  $a$  moves away increasing the gap size. If a viscous (continually fed) accretion disk is present outside the binary in place of the annular ring, the response of the disk is determined by the competition between the tidal torque exerted by the binary and the pressure and/or viscous torques present inside the disk that, in opposition to the tide, tend to refill the emptied region and keep the gap closed. A hollow, low density region (the gap) of size  $\Delta \gtrsim a$ , surrounding the binary, forms as long as  $\Delta$  is larger than the Roche lobe radii, i.e. the radii of the two equipotential surfaces connecting the two black holes ( $\Delta > R_{\text{RL}}$ ), and the disk scale height  $H < \Delta$ . The gap is maintained when the gap-closing time  $\Delta t_{\text{close}}$ , comparable in magnitude to the viscous/turbulence time at the inner edge of the disk  $\sim t_{\text{vis/turb}}(a) \sim \Delta/v_{\text{drift/turb}}$  (where  $v_{\text{drift/turb}}$  is the radial drift/turbulent velocity of the disk near  $a$ ) is longer than the gap-opening time  $\Delta t_{\text{open}} \sim \Delta L/T$ , where  $\Delta L \sim (\rho_{\text{gas}} H \Delta^2) R V_{\text{cir}}$  is the angular momentum that must be added to the gas to open a gap of size  $\Delta$ , and  $T$  is the tidal torque by dynamical friction that can be estimated as  $T \sim R F_{\text{DF}}^{\text{gas}} \sim R 4\pi \ln \Lambda \rho_{\text{gas}} (GM_{\text{BH,T}}/V_{\text{cir}})^2$  (from eq. 10). The condition  $\Delta t_{\text{close}} > \Delta t_{\text{open}}$  is fulfilled in presence of a massive binary, i.e. whenever the gas mass enclosed within  $\sim a$  (estimated before gap opening)  $M_{\text{gas}}(a) \lesssim 0.5 M_{\text{BH,T}}$ , as demonstrated in numerical simulations<sup>157</sup>.

Figure 12 shows the outcome of an SPH simulation (performed using GADGET-2<sup>175</sup>) designed by Cuadra et al.<sup>176</sup> to follow the early dynamical evolution of a black hole binary inside a circum-binary ring in Keplerian rotation and with initial profile  $\Sigma = \Sigma_0(R_0/R)$ . The gap, already present as initial condition, is maintained for the entire duration of the simulation ( $\sim 1200$  dynamical times  $t_{\text{dyn}}$ ) as gas piles up near  $R \sim 3a$  in response to the joint action of the tidal torque offered by the binary and of the torques in the fluid. The binary soon starts to decay and to increase its eccentricity. With time however, as illustrated in Figure 12, the ring, allowed to cool on a few dynamical times, becomes unstable to non-axisymmetric perturbations that are transmitted through the entire structure. The ring thus spreads over a larger volume. At this point the action of viscous torques becomes progressively ineffective and the binary stalls. Whether the binary continues to decay on a much longer timescale is still matter of a debate, the process being reminiscent to that of planet *migration* in circum-stellar disks<sup>170–174</sup>.

Analytical and numerical studies of black hole migration in standard Keplerian accretion disks<sup>174,177–181</sup> have indicated that migration is a slow process occurring on a timescale longer than the viscous time  $t_\nu$  at the inner edge of the disk where the gap is located ( $R_{\text{gap}} \sim 2a$ ). If  $\Sigma_{\text{gap}}$  is the unperturbed surface density of a reference Keplerian disk at  $R_{\text{gap}}$  and  $M_{\text{gap}} = 2\pi R_{\text{gap}}^2 \Sigma_{\text{gap}}$  the mass enclosed, the resulting migration time is crudely,  $t_{\text{migration}} \sim (M_{\text{BH,T}}/M_{\text{gap}})t_\nu$ .

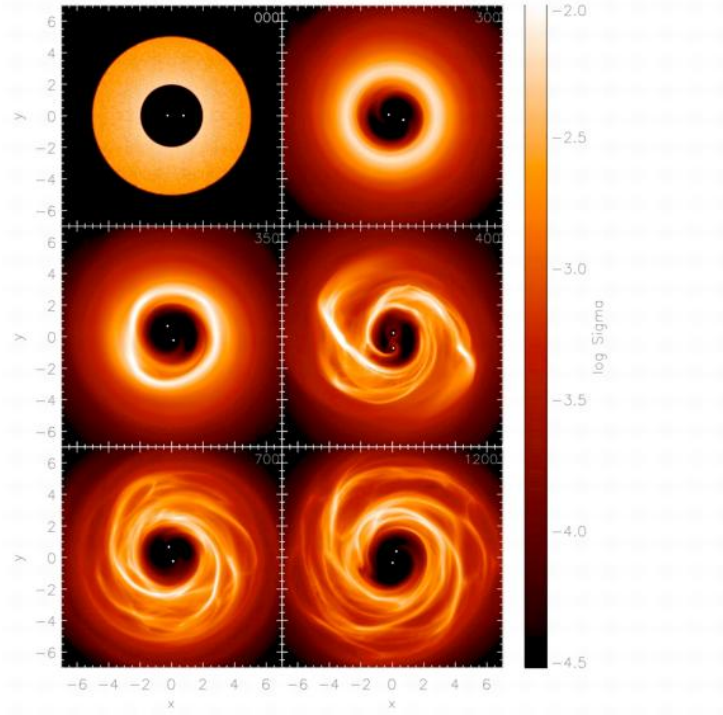


Figure 12: Evolution of a black hole binary in a circum-binary ring, as simulated by Cuadra et al.<sup>176</sup>. The Figure shows the logarithmic maps of the disk column density at different times, and the white dots indicate the current position of the black holes. The panel at  $t = 0$  shows the smooth initial condition. Until  $t \sim 350\Omega_0^{-1}$  (where  $\Omega_0$  is the Keplerian frequency of the binary at its initial orbital separation  $a_0$ ) material piles up at a distance comparable to  $\sim 3a_0$ , as a result of the gravitational torques: the accretion disk responds to the tidal field of the binary increasing its surface density at radii nearest to the black holes. The ring breaks due to its self-gravity, spreading its gas over the original radial range. Stationary spiral patterns develop until the simulation ends. The binary has mass ratio  $q_{\text{BH}} = 0.3$  and the disk mass is  $M_{\text{disk}} = 0.2M_{\text{BH,T}}$ .

Cuadra et al.<sup>176</sup> computed the migration time  $t_{\text{migration}}$  in a self-regulated ( $Q \sim 1$ ) circum-binary disk, starting from an estimate of  $t_\nu$  based on a viscosity prescription that originates from self-gravity, and from an appropriate estimate of the cooling time and of the opacity law of the gas in the disk. Since  $t_{\text{migration}}$  is found to be proportional to  $\Sigma_{\text{gap}}^{-b}$  (with  $b > 0$ ), the maximum rate of orbital decay can be inferred considering the highest  $\Sigma_{\text{gap}}$  consistent with a Toomre parameter  $Q \sim 1$ . (Denser disks would likely fragment into stars rather than remaining gaseous and this would destroy the hydrodynamical interaction that leads to black hole binary migration.) Following Cuadra et al., binaries with mass  $M_{\text{BH,T}} < 10^7 M_\odot$ , i.e. binaries in the frequency interval of *LISA* operation, are found to have migration times  $t_{\text{migration}} \sim 10^{8-9}$  yr, while heavier binaries would instead stall, and/or decay via three-body encounters off stars<sup>125</sup>.

If migration, as described in<sup>176–179</sup>, continues down to smallest scales, the circum-binary disk is no longer dominated by self-gravity and takes the form of a Keplerian accretion disk. In this regime, the binary-disk interaction is better described in terms of a sequence of *resonances*<sup>181</sup>. Azimuthal and longitudinal modes at the outer Lindblad resonance are excited that promote the orbital decay of the binary. Whether black hole migration is conducive to the domain in which gravitational waves take over and guide the inspiral is still uncertain. Should this occur, then below  $a_{\text{GW}}$  the circum-binary disk would become no longer dynamically important. Only gravitational waves are expected to influence the orbital elements: waves circularize the orbit and if  $e$  is large at the end of black hole migration, the two black holes may coalesce with still a residual eccentricity which is imprinted in the gravitational wave pattern<sup>182</sup>.

The presence of the circum-binary accretion disk and of circum-stellar disks around each black hole, unimportant at dynamical level during the GW phase, can play a key role in determining whether the gravitational wave signal from the binary is accompanied by a bright electromagnetic counterpart. This will be the subject of next Section.

## 6 Preglow and Afterglow of coalescence events

Consider a black hole binary crossing the  $\text{H} \rightarrow \text{GW}$  boundary. After a time  $t_{\text{GW}}$  it will then coalesce becoming one of the loudest sources of gravitational waves observable in the whole sky with *LISA*. *LISA* will operate as an all-sky monitor, detecting at the same time galactic and cosmological sources. Given the difficulty to disentangle the different signals, and the large number of noise sources, the accuracy in determining a single source position is still matter of debate. A distinctive electromagnetic counterpart to a *LISA* detection of a black hole coalescence would have different payoffs, allowing to identify the galaxy host, and to observe directly the redshift of the source. As a consequence, the simultaneous detection of a gravitational wave and an electromagnetic signal could be used to estimate fundamental cosmological parameters as coalescing binaries are standard *sirens*<sup>183</sup>. Detection of an electromagnetic counterpart would also improve our understanding of the accretion physics of massive black holes, by comparing directly the luminosity with the black hole’s masses and spins obtained directly from the gravitational wave signal. A large number of possible electromagnetic counterparts have been proposed in the last few years (see, e.g., Kocsis & Loeb<sup>184</sup> and references therein). In this review we will discuss only few selected candidates, in relation to the dynamical evolution of the black holes during (the preglows) and after (the afterglows) coalescence.

## 6.1 Preglows

As already discussed, the dynamical effect of a massive black hole binary is to open a gap in its circum-binary accretion disk. As the binary semi-major axis decays due to the interaction with the disk itself, viscous dissipation maintains the outer edges of the gap at  $R_{\text{gas}} \sim 2a$ . Only during the last phases of binary evolution, when the semi-major axis decays due to gravitational wave emission, the outer disk and binary evolution decouples. The distance between the black holes and the inner rim of the circum-binary disk (still moving toward the center on the viscous timescale) increases. If an accretion disk is present, in addition, around the primary black hole (of an unequal mass binary), the secondary creates the conditions for excavating an *annular* gap, i.e. a hollow region between the circum-stellar disk around the primary and the outer circum-binary disk. As a consequence, the gas orbiting at radii smaller than the outer edge of the inner circum-stellar disk is driven inward under the action of gravitational torques by the inspiraling secondary black hole. Armitage & Natarajan<sup>185</sup> showed that this effect amplifies the accretion rate onto the primary that can largely exceed the Eddington limit just prior coalescence. They suggested that a large fraction of the energy associated with this extreme pre-coalescence accretion event is converted in thermal energy of the gas accreting onto the primary. The increased temperature triggers large outflows of gas, with velocities comparable to the orbital velocity of  $\sim 10^4 \text{ km s}^{-1}$ . The authors suggest that such strong high velocity outflows can be viewed as clear signal of coalescing or recently coalesced black hole binaries.

## 6.2 Afterglows

Armitage & Natarajan<sup>185</sup> showed that the evolution of the inner edge of the gap causes a possibly observable preglow just before coalescence. In this section we discuss the consequences of the evolution of the outer edge of the gap, resulting in an afterglow observable years after coalescence.

When the black holes reach coalescence, the circum-binary disk is free from gravitational torques and starts to spread inwards viscously refilling the gap. Milosavljevic & Phinney<sup>186</sup> estimated that the timescale before complete refilling of the gap and the turn-on of observable accretion activity is  $\sim 7(1+z)(M/10^6 M_\odot)^{1.32}$  yr. They also constrained the luminosity and spectrum of the turning-on AGN associated to the binary coalescence event:  $\sim 10^{43.5}(M/10^6 M_\odot) \text{ erg s}^{-1}$  are emitted between 0.5–2 keV in the rest frame of the source and for hole’s masses in the *LISA* band. Based on models of the black hole assembly<sup>29,30,110</sup>, Dotti et al.<sup>187</sup> estimated that next generation X-ray missions (such as *XEUS* or *Constellation-X*) will be able to detect an X-ray afterglow for a large fraction of the total coalescences detectable by *LISA* in three years of operation ( $\sim 9, 21, \text{ and } 28$  after 1, 5, and 20 yr from the GW detection, respectively).

## 6.3 Kick-induced Shocks in circum-binary disks

Black hole binaries recoil, at the time of their coalescence, due to anisotropic emission of gravitational waves. The possibility that recoiling black holes can produce an observable electromagnetic signature of a recent coalescence, already suggested by Milosavljevic & Phinney<sup>186</sup>, has been subject of a detailed discussion only recently.

Lippai, Frei & Haiman<sup>188</sup> simulated the response of a thin disk, initially orbiting around a  $10^6 M_\odot$  black hole, to kicks that eject the black hole from the center. In particular they explored the range  $500 \text{ km s}^{-1} < v_{\text{rec}} < 4000 \text{ km s}^{-1}$ , where  $v_{\text{rec}}$  is the kick velocity of the black hole recoiling either in the disk plane or perpendicular to the disk. The perturbation in the potential well exerted by the black hole recoiling in the disk plane alters

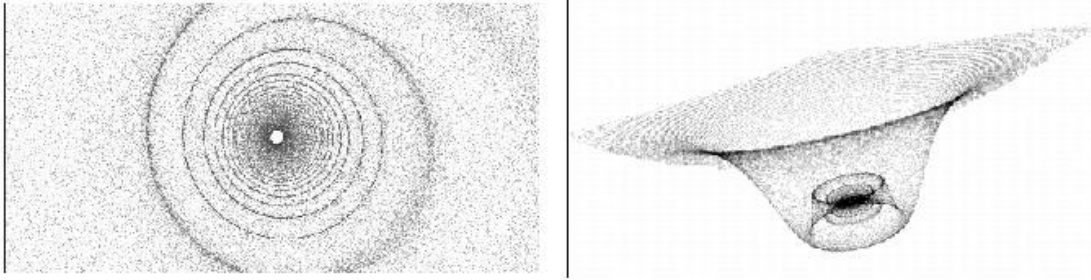


Figure 13: Output of two different runs presented in Lippai et al.<sup>188</sup>. Left panel: face-on view of the perturbations triggered in the accretion disk by a black hole recoiling in the disk plane. The snapshot shows the output of a simulation with  $v_{\text{rec}} = 500 \text{ km s}^{-1}$ , 90 days after the kick. Light shades correspond to regions of unperturbed density, while dark shades to regions  $\sim 10$  times over-dense. Right panel: areal view of a disk perturbed by a black hole recoiling perpendicularly to the disk. The snapshot is taken after 1 week, and  $v_{\text{rel}} = 500 \text{ km s}^{-1}$ . In this case, the density enhancement is noticeably weaker than the one observed in the coplanar simulation,  $\sim 10\%$  of the initial value.

the orbits of the particles forming the disk, resulting in the formation of over-density regions distributed over a tightly wound spiral caustic, as shown in the left panel of Figure 13. The density enhancement within weeks after the ejection, can be more than 10 times larger than the unperturbed disk, and moves outward at the speed  $v_{\text{rec}}$ . Density enhancements are observed also for black holes recoiling perpendicularly to the disk plane (see Figure 13, right panel), but are much weaker ( $\sim 10\%$  of the unperturbed value), and develops in caustic only after  $\gtrsim 1 \text{ yr}$ . Assuming that the gas forming the density enhancement is shocked-heated, the authors estimated a prompt increase in the emitted luminosity up to  $L_{\text{rec}}/L_{\text{Ed}} \sim 6.3 \times 10^{-4} (1.6 \times 10^{-2})$ , 70 days ( $\sim 2 \text{ yr}$ ) after the coalescence. Lippai et al. found also that the converging velocity ( $v_{\text{conv}}$ ) of the shocking regions is an increasing function of the radius, so that the spectrum of the afterglow peaks at a characteristic photon energy  $k_B T_{\text{shock}} \propto v_{\text{conv}}^2 \sim 3 \text{ eV}$  50 days after coalescence, and grows up to  $\sim 50 \text{ eV}$   $\sim 2 \text{ yr}$  after. Schnittman & Krolik<sup>189</sup> noticed that the disk considered in Lippai et al.<sup>188</sup> is optically thick, and as a consequence the radiation is absorbed and re-emitted with a thermal spectrum in the infrared. They also applied their results to cosmological models of structure formation, finding that  $\sim 1 - 10$  of these afterglows should be detectable in the *Spitzer*, *XMM-Newton*, and *Chandra* surveys.

#### 6.4 Recoiling black holes in galaxy remnants

The presence of a recoiling black hole ejected from its nucleus can be observed in galaxy merger remnants up to  $10^8 \text{ yr}$  after the binary coalescence. Different electromagnetic signatures have been proposed: the recoiling black hole can be observed as an off-center QSO, if the hole itself is able to retain a punctured disk at the coalescence<sup>46</sup>. Volonteri & Madau<sup>47</sup> studied this process in a statistical context, finding that tens of off-centered AGNs should be discovered by the future *James Webb Space Telescope (JWST)*. Episodic accretion flares can be produced from the tidal disruption of stars during the lifetime of the recoiling black hole<sup>190,191</sup>.

A recoiling massive black hole can also retain a “hyper-compact stellar system” (HCSS) detectable in the optical as a luminous cluster<sup>190,192</sup>. The structural properties of HCSSs are defined by the stellar distribution

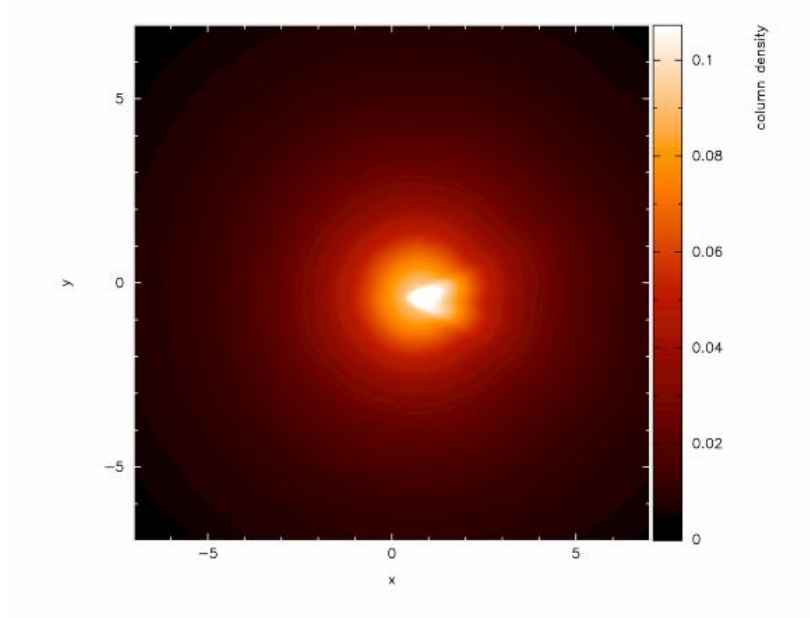


Figure 14: Recoiling black hole in a massive elliptical galaxy model<sup>193</sup>. The figure shows the color-coded density map (in logarithmic scale) of the gas perturbed by the massive black hole on its return orbit, at its first pericentric passage. The recoiling black hole (of  $6 \times 10^9 M_{\odot} \sim 6 \times 10^{-3} M_{\text{galaxy}}$ ) is ejected with an initial  $v_{\text{rec}} = 900 \text{ km s}^{-1}$  ( $\mathcal{M} \sim 3$ ), and is moving on the plane perpendicular to the line of sight. The box is 14 kpc aside.



function of stars near the black holes prior coalescence, and by the recoil velocity of the black hole remnant<sup>192</sup>. The authors estimate that the size and luminosity of HCSSs is similar to that of a globular cluster, but can reach values typical of ultra-compact dwarf galaxies if the host galaxies are very massive and the kick velocities sufficiently small. HCSSs are distinguishable from globular clusters and dwarf galaxies because of the peculiar velocity distribution of their stars: the internal velocities in a HCSS are comparable to the recoil velocity, allowing for velocity dispersions much larger than the ones observed in canonical globular clusters. The authors use cosmological models to constrain the number of HCSSs observable in the local universe, finding that up to 100 HCSSs should be present in the Virgo cluster, even if only a few could be bright enough to be confirmed as HCSSs by spectroscopical follow-ups.

A different signature of a recoiling black hole has been discussed in Devecchi et al.<sup>193</sup>. The authors perform N-Body/SPH simulations of black holes recoiling in massive elliptical galaxies, hosting a hot, X-ray emitting, gas component. They discover that the gravitational interaction between the moving black hole and the hot medium excites a density perturbation in the gas, observable as enhancement in the X-ray emission. If the black hole is moving with a subsonic speed, a nearly spherical distribution of hot particles forms around: this feature can live up to  $\sim 10^8$  yr. If the black hole is moving supersonically, it triggers an over-density in the form of a Mach cone, as illustrated in Figure 14, observable for few tens of Myr. The possibility to observe these features (the spherical or conical X-ray enhancement) depends strongly on the angular resolution of the X-ray detector. Thanks to the high spatial resolution, *Chandra* can detect recoiling black holes out to the distance of Virgo.

## 7 Outstanding problems and conclusions

The problem of formation and coalescence of dual black holes in merging galaxies goes back to the influential paper of Begelman, Blandford & Rees<sup>99</sup>. Since then, our view on the formation of cosmic structures and of their embedded black holes has improved dramatically. We are now aware of the fact that dual, binary and recoiling quasars are exclusive signposts of the process of galaxy assembly. Their search in survey covering the entire electromagnetic spectrum has then become compelling, as compelling is a deep understanding of the dynamics of their formation, at theoretical level.

This review has touched key aspects of the long journey traveled by the black holes on their path to coalescence, highlighting its complexity. The processes that are conducive, in merging galaxies, to black hole coalescence are heterogeneous as the physical/dynamical range that needs to be covered is enormous, going from the scale of a cosmic merger ( $\sim 100$  kpc) down to the tiny volume of a galaxy's nuclear region of  $\sim 10^{-3}$  pc. Only below this small scale, gravitational waves alone drive the black hole to coalescence. Given the complexity of the problem, a step ahead has been carried out in recent years thanks to major advances in numerical simulations. Despite this effort there is no simulation at present that is capable of following the pairing process in full realism, either in pure stellar/gas-poor as well as in gas-rich environments, from self-consistent cosmological conditions.

In stellar backgrounds there is still the need to explore in greater detail loss cone refilling in the time-varying non-axisymmetric gravitational potentials that form in the aftermath of a merger, and the role of instabilities and of massive perturbers created in situ. On a smaller scale, when few body interactions become important, there is also the need to include post-Newtonian black hole dynamics, as indicated in in a recent study<sup>194</sup>. In gas-rich backgrounds, dissipation is known to play a key role in speeding black hole inspiral, but often

the thermodynamical description of the gas has been treated in simple, idealized terms: the gas is multi-phase and star formation, together with stellar/AGN feedback may play a critical role in affecting the actual dynamics of the black holes. The inclusion of these composite effects is a must for the future, and we are working on these lines. Low mass black holes at high redshifts are likely to pair in gas-rich halos, while high mass black holes at lower redshifts likely pair in gas-poor stellar backgrounds. Thus exploring the dynamics in different habitat is of major importance.

The search of dual, binary and recoiling black holes, fed through accretion, will continue: imaging of galaxies in close interaction may unveil the presence of pairing black holes on kpc scales. Spectroscopically, the presence of large Doppler displacements in the emission line systems of quasars and AGNs<sup>78,79,82</sup> may reveal the presence of black holes in close orbital motion on scales close to a parsec. A major advance will come from *LISA* in space and the Pulsar Timing Array experiment on Earth. Pulsar Timing Array will detect the emission of very massive black holes many year before coalescence ( $< 10^6$  yr), while *LISA* will detect the last year of inspiral and the final rapid coalescence. Thus, we have tools to trace the entire dynamical evolution of black holes using both the electromagnetic and gravitational wave windows.

### Acknowledgements

We thank all the people that have had a long term collaboration with the authors and contributed to many of the results discussed in this review; Simone Callegari, Roberto Decarli, Bernadetta Devecchi, Fabio Governato, Francesco Haardt, Stelios Kazantzidis, George Lake, Piero Madau, Lucio Mayer, Carmen Montuori, Ben Moore, Tom Quinn, Alberto Sesana, Joachim Stadel, Marta Volonteri, and James Wadsley.

### References

- [1] J. Kormendy and D. Richstone, *ARA&A* 33, 581 (1995)
- [2] J. Magorrian et al., *AJ* 115, 2285 (1998)
- [3] A. Marconi and L. K. Hunt, *ApJ*, 589, L21 (2003)
- [4] N. Häring and H. W. Rix, *ApJ* 604, L89 (2004)
- [5] K. Gebhardt et al., *AJ* 119, 1157 (2000)
- [6] L. Ferrarese and D. Merritt, *ApJ* 539, L9 (2000)
- [7] L. Ferrarese and H. Ford, *Space Science Reviews* 116, 523 (2005)
- [8] G. L. Granato, G. De Zotti, L. Silva, A. Bressan, and L. Danese, *ApJ* 600, 580 (2004)
- [9] T. Di Matteo, V. Springel, and L. Hernquist, *Nature* 433, 7026, 604 (2005)
- [10] P. F. Hopkins, L. Hernquist, T. J. Cox, and D. Keres, *ApJS* 175, 356 (2008)
- [11] T. Di Matteo, J. Colberg, V. Springel, L. Hernquist, and D. Sijacki, *ApJ* 676, 33 (2008)
- [12] P. Madau and M. J. Rees, *ApJ* 551, L27, (2001)

- [13] M. G. Haehnelt and M. J. Rees, MNRAS 263, 168, **(1993)**
- [14] A. Loeb and F. A. Rasio, ApJ 432, 52, **(1994)**
- [15] D. J. Eisenstein and A. Loeb ApJ 443, 11, **(1995)**
- [16] V. Bromm and A. Loeb, *Nature* 425, 812, **(2003)**
- [17] S. M. Koushiappas, J. S. Bullock, and A. Dekel, MNRAS 354, 292, **(2004)**
- [18] M. C. Begelman, M. Volonteri, and M. J. Rees, MNRAS 370, 289, **(2006)**
- [19] G. Lodato and P. Natarajan, MNRAS 371, 1813, **(2006)**
- [20] B. Devecchi and M. Volonteri, ApJ 694, 302 **(2009)**
- [21] A. Soltan, MNRAS, 200, 115 **(1982)**
- [22] A. Merloni and S. Heinz, MNRAS 388, 1011 **(2008)**
- [23] X. Fan et al., AJ 122, 1833, **(2001)**
- [24] L. C. Ho, Carnegie Observatories Astrophysics Series, Volume 1: *Coevolution of Black Holes and Galaxies*, Cambridge University Press **(2004)**
- [25] M. Colpi, V. Gorini, F. Haardt, U. Moschella, Book Review: *Joint evolution of black holes and galaxies*, Taylor & Francis **(2006)**
- [26] D. Hils and P. Bender, ApJ, 447, L7 **(1995)**
- [27] A. H. Jaffe and D. C. Backer, ApJ 583, 616 **(2003)**
- [28] J. S. B. Wyithe and A. Loeb, ApJ 590, 691 **(2003)**
- [29] A. Sesana, F. Haardt, P. Madau, and M. Volonteri, ApJ 611, 623 **(2004)**
- [30] A. Sesana, F. Haardt, P. Madau, and M. Volonteri, ApJ 623, 23 **(2005)**
- [31] A. Alcubierre et al., Phys Rev. D 72, 044004 **(2005)**
- [32] F. A. Jenet, A. Lommen, S. L. Larson, and L. Wen, ApJ 606, 799 **(2004)**
- [33] F. A. Jenet, T. Creighton, and A. Lommen, ApJ 627, L125 **(2005)**
- [34] A. Sesana, A. Vecchio, and C. N. Colacino, MNRAS 390, S192 **(2008)**
- [35] F. Pretorius, Lecture note in *Physics of Relativistic Objects in Compact Binaries: from Birth to Coalescence*, Edited by M. Colpi, P. Casella, V. Gorini, U. Moschella and A. Possenti., Astrophysics and Space Science Library, Vol. 359. Berlin: Springer **(2009)** (arXiv0710.1338P)
- [36] A. Vecchio, Phys. Rev. D 70, 042001 **(2004)**
- [37] R. N. Lang and S. A. Hughes, Phys Rev. D 74, 122001 **(2006)**

- [38] J. A. González, U. Sperhake, B. Bruggmann, M. Hannam, and S. Husa, *Phys. Rev. Lett.* 98, 091101 (2007)
- [39] F. Herrmann, I. Hinder, D. M. Shoemaker, P. Laguna, and R. A. Matzner, *Phys. Rev. D* 76, 084032 (2007)
- [40] M. Campanelli, C. Lousto, Y. Zlochower, and D. Merritt, *ApJ* 659, L5 (2007)
- [41] M. Campanelli, C. Lousto, Y. Zlochower, and D. Merritt, *Phys. Rev. Lett.* 98, 1102 (2007)
- [42] J. D. Schnittman and A. Buonanno, *ApJ* 662, L63 (2007)
- [43] J. G. Baker, W. D. Boggs, J. Centrella, B. J. Kelly, S. T. McWilliams, M. C. Miller, and J. R. van Meter, *ApJ* 682, L29 (2008)
- [44] P. C. Peters, *Phys. Rev. B* 136, 1224 (1964)
- [45] P. Madau and E. Quataert, *ApJ* 606, L17 (2004)
- [46] A. Loeb *Phys. Rev. Lett.* 99, 041103 (2007)
- [47] M. Volonteri and P. Madau, *ApJ* 687, L57 (2008)
- [48] F. N. Owen, C. P. O’Dea, M. Inoue, and J. A. Eilek, *ApJ* 294, L85 (1985)
- [49] M. Yokosawa and M. Inoue, *PASJ* 37, 655 (1985)
- [50] T. C. Beers, K. Gebhardt, J. P. Huchra, W. Forman, C. Jones, and G. D. Bothun, *ApJ* 400, 410 (1992)
- [51] D. S. Hudson, T. H. Reiprich, T. E. Clarke, and C. L. Sarazin, *A&A* 453, 433 (2006)
- [52] D. Guidetti, M. Murgia, F. Govoni, P. Parma, L. Gregorini, H. R. de Ruiter, R. A. Cameron, and R. Fanti, *A&A* 483, 699 (2008)
- [53] J. W. Fried and H. Ulrich, *A&A* 152, L14 (1985)
- [54] K. Iwasawa and A. Comastri, *MNRAS* 297, 1219 (1998)
- [55] P. Vignati et al., *A&A* 349, L57 (1999)
- [56] L. J. Tacconi, R. Genzel, M. Tecza, J. F. Gallimore, D. Downes, and N. Z. Scoville, *ApJ* 524, 732 (1999)
- [57] M. Tecza, R. Genzel, L. J. Tacconi, S. Anders, L. E. Tacconi-Garman, and N. Thatte, *ApJ* 537, 178 (2000)
- [58] S. Komossa, V. Burwitz, G. Hasinger, P. Predehl, J. S. Kaastra, and Y. Ikebe, *ApJ* 582, L15 (2003)
- [59] F. Eisenhauer et al., *Astron. Nachr.* 325, 120 (2004)
- [60] L. Armus et al., *ApJ* 640, 204 (2006)
- [61] C. E. Max, G. Canalizo, and W. H. de Vries, *Science* 316, 1877 (2007)
- [62] S. Bianchi, M. Chiaberge, E. Piconcelli, M. Guainazzi, and G. Matt, *MNRAS* 386, 105 (2008)

- [63] R. Della Ceca et al., ApJ 581, L9 (2002)
- [64] L. Ballo, V. Braitto, R. della Ceca, L. Maraschi, F. Tavecchio, and M. Dadina, ApJ 600, 634 (2004)
- [65] M. García-Marín, L. Colina, S. Arribas, A. Alonso-Herrero, and E. Mediavilla, ApJ 650, 850 (2006)
- [66] M. Imanishi and K. Nakanishi, PASJ 58, 813 (2006)
- [67] A. Tarchi, P. Castangia, C. Henkel, and K. M. Menten, New AR 51, 67 (2007)
- [68] A. J. Barth, M.C. Bentz, J. E. Greene, and L. C. Ho, ApJ 683, L119 (2008)
- [69] H. L. Maness, G. B. Taylor, R. T., Zavala, A. B. Peck and L. K. Pollack, ApJ 602, 123 (2004)
- [70] C. Rodriguez, G. B. Taylor, R. T., Zavala, A. B. Peck, L. K. Pollack, and R. W. Romani, ApJ 646, 49 (2006)
- [71] B. Morganti, R. Emonts, J. Holt, C., Tadhunter, T. Oosterloo, and C. Struve, Astron. Nachr. 330, 233 (2009)
- [72] C. Rodriguez, G. B. Taylor, R. T., Zavala, Y. M., Pihlstrom, and A. B. Peck, ApJ in press (arXiv:0902.4444) (2009)
- [73] H. J. Lehto and M. J. Valtonen, ApJ 460, 207 (1996)
- [74] M. J. Valtonen et al., ApJ 646, 36 (2006)
- [75] M. J. Valtonen et al., *Nature* 452, 851 (2008)
- [76] J. K. Adelman-McCarthy et al., ApJ 172, S634 (2007)
- [77] S. Komossa, H. Zhou, and H. Lu, ApJ 678, L81 (2008)
- [78] T. Bogdanovic, M. Eracleous, and S. Sigurdsson, ApJ in press (arXiv:0809.3262) (2009)
- [79] M. Dotti, C. Montuori, R. Decarli, M. Volonteri, M. Colpi, and F. Haardt, submitted to MNRAS (arXiv:0809.3446) (2009)
- [80] T. M. Heckman, J. H. Krolik, S. M. Moran, J. Schnittman and S. Gezari, ApJ 695, 363 (2009)
- [81] G. A. Shields, E. W. Bonning, and S. Salviander, ApJ in press (arXiv:0810.2563) (2009)
- [82] T. A. Boroson and T. R. Lauer, *Nature* 458, 53 (2009)
- [83] A. Toomre, in *The Evolution of Galaxies and Stellar Populations*, Ed. B. M. Tinsley & R. B. Larson (New Haven: Yale Univ. Observatory), 401 (1977)
- [84] A. Toomre and J. Toomre, ApJ 178, 623 (1972)
- [85] S. D. White and M. J. Rees, MNRAS 183, 341 (1978)
- [86] J. Kormendy, D. B. Fisher, M. E. Cornell, and R. Bender, ApJS in press (arXiv:0810.1681) (2009)
- [87] J. Kormendy and R. Bender, ApJ 691, L142 (2009)

- [88] S. M. Faber et al., AJ 114, 1771 (1997)
- [89] P. F. Hopkins, J. T. Cox, Thomas, S. N. Dutta, L. Hernquist, J. Kormendy, and T. R. Lauer, ApJS 181, 135 (2009)
- [90] P. F. Hopkins, T. R. Lauer, T. J. Cox, L. Hernquist, and J. Kormendy, ApJ in press (arXiv:0806.2325) (2009)
- [91] M. Milosavljević, M. and D. Merritt, D. ApJ 563, 34 (2001)
- [92] M. Milosavljevic, D. Merritt, A. Rest, and F. C. van den Bosch, MNRAS 331, 51 (2002)
- [93] D. Merritt, ApJ 648, 976 (2006)
- [94] D. Merritt, S. Mikkola, and A. Szell, ApJ, 671, 53 (2007)
- [95] D. Merritt, M. Milosavljević, M. Favata, S. A. Hughes, and D. E. Holz, ApJ 607, L9 (2004)
- [96] M. Boylan-Kolchin, C. P. Ma, and E. Quataert, ApJ 613, L37 (2004)
- [97] A. Gualandris and D. Merritt, ApJ 678, 780 (2008)
- [98] T. Bogdanovic, C. S. Reynolds, and M. C. Miller, ApJ 661, L147 (2007)
- [99] M. C. Begelman, R. D. Blandford, and M. J. Rees, *Nature* 287, 307 (1980)
- [100] F. Governato, M. Colpi, and L. Maraschi, MNRAS 271, 317 (1994)
- [101] M. Milosavljevic and D. Merritt, ApJ 563, 34 (2001)
- [102] Q. Yu, MNRAS 331, 931 (2002)
- [103] J. Makino and Y. Funato, ApJ 602, 93 (2004)
- [104] A. Sesana, F. Haardt, and P. Madau, ApJ 660, 546 (2007)
- [105] W. H. Press and P. Schechter, ApJ 187, 425 (1974)
- [106] C. Lacey and S. Cole, MNRAS 262, 627 (1993)
- [107] G. Kauffmann and M. G. Haehnelt MNRAS 311, 576 (2000)
- [108] G. Kauffmann and M. G. Haehnelt, MNRAS 332, 529 (2003)
- [109] T. Di Matteo, R. A. C. Croft, V. Springel, and L. Hernquist, ApJ 593, 56 (2003)
- [110] M. Volonteri, F. Haardt, and P. Madau, ApJ 582, 559 (2003)
- [111] J. M. Bromley, R. S. Somerville, and A. C. Fabian, MNRAS 350, 456 (2004)
- [112] V. Springel et al., *Nature* 435, 629 (2005)
- [113] M. Volonteri, G. Lodato, and P. Natarajan, MNRAS 383, 1079 (2008)
- [114] S. Chandrasekhar, ApJ 97, 255 (1943)

- [115] M. Colpi and A. Pallavicini, ApJ 502, 150 (1998)
- [116] M. Colpi, L. Mayer, and F. Governato, ApJ 525, 720 (1999)
- [117] H. E. Kandrup, ApJ 244, 316 (1981)
- [118] J. D. Bekenstein and E. Maoz, ApJ 390, 79 (1992)
- [119] E. C. Ostriker, ApJ 513, 252 (1999)
- [120] D. Merritt and M. Milosavljević: *Living Reviews in Relativity*, vol. 8, no. 8 (2005)
- [121] M. Milosavljević and D. Merritt, AIP Conference Proceedings, 686, 201 (2003)
- [122] V. Springel, N. Yoshida, and S. D. M. White, New Astron. 6, 79 (2001)
- [123] R. Spurzem, J. Comput. Appl. Math. 109, 407 (1999)
- [124] A. Escala, R. B. Larson, P. S. Coppi, and D. Maradones, ApJ 607, 765 (2004)
- [125] M. Milosavljevic and D. Merritt, ApJ 596, 860 (2003)
- [126] P. Berczik, D. Merritt, and R. Spurzem, ApJ 633, 680 (2005)
- [127] D. Merritt and M. Y. Poon, ApJ 606, 788 (2004)
- [128] P. Berczik, D. Merritt, R. Spurzem, and H. P. Bischof, ApJ 642, L21 (2006)
- [129] A. Sesana, F. Haardt, and P. Madau, ApJ 660, 546 (2007)
- [130] H. B. Perets, C. Hopman, and T. Alexander, ApJ 656, 709 (2007)
- [131] H. B. Perets and T. Alexander, ApJ 677, 146 (2008)
- [132] A. Sesana, F. Haardt, and P. Madau, ApJ 686, 432 (2008)
- [133] J. Makino and T. Ebisuzaki, ApJ, 436, 607 (1994)
- [134] M. J. Valtonen, MNRAS 278, 186 (1996)
- [135] O. Blaes, M. H. Lee, and A. Socrates, ApJ 578, 775 (2002)
- [136] I. Shlosman, J. Frank, and M. C. Begelman, *Nature* 338, 45 (1989)
- [137] A. Escala, ApJ 671, L31 (2007)
- [138] S. Kazantzidis, L. Mayer, M. Colpi, P. Madau, V. P. Debattista, J. Wadsley, J. Stadel, T. Quinn, and B. Moore, ApJ 623, L67 (2005)
- [139] P. F. Hopkins, L. Hernquist, P. Martini, T. J. Cox, B. Robertson, T. Di Matteo, and V. Springel, ApJ 625, L71 (2005)
- [140] P. F. Hopkins, L. Hernquist, T. J. Cox, T. Di Matteo, B. Robertson, and V. Springel, ApJS 163, 1 (2006)

- [141] L. Mayer, S. Kazantzidis, P. Madau, M. Colpi, T. Quinn, and J. Wadsley, *Science* 316, 1874 (2007)
- [142] J. F. Navarro, C. S. Frenk, and S. D. M. White, *ApJ* 490, 493 (1997)
- [143] J. W. Wadsley, J. Stadel, and T. Quinn, *New Astron.* 9, 137 (2004)
- [144] M. Spaans and J. Silk, *ApJ* 538, 115 (2000)
- [145] R. S. Klessen, M. Spaans. and A. Jappsen, *MNRAS* 374, L29 (2007)
- [146] D. Downes and P. M. Solomon, *ApJ* 507, 615 (1998)
- [147] R. I. Davies, L. J. Tacconi, and R. Genzel, *ApJ* 602, 148 (2004)
- [148] R. I. Davies, L. J. Tacconi, and R. Genzel, *ApJ* 613, 781 (2004)
- [149] T. R. Greve, P. P. Papadopoulos, Y. Gao, and S. J. E. Radford, *ApJ* 692, 1432 (2009)
- [150] V. Springel, T. Di Matteo, and L. Hernquist, *ApJ* 620, L79 (2005)
- [151] V. Springel, T. Di Matteo, and L. Hernquist, *MNRAS* 361, 776 (2005)
- [152] K. Wada and C. A. Norman, *ApJ* 547, 172 (2001)
- [153] M. Boylan-Kolchin, C. Ma, and E. Quataert, *MNRAS* 362, 184 (2005)
- [154] M. Boylan-Kolchin, C. Ma, and E. Quataert, *MNRAS* 369, 1081 (2006)
- [155] M. Boylan-Kolchin and C. Ma, *MNRAS* 374, 122 (2007)
- [156] S. Callegari, L. Mayer, S. Kazantzidis, M. Colpi, F. Governato, T. Quinn, and J. Wadsley, submitted to *ApJL* (arXiv:0811.0615)
- [157] A. Escala, R. B. Larson, P. S. Coppi, and D. Maradones, *ApJ* 630, 152 (2005)
- [158] M. Dotti, M. Colpi, and F. Haardt, *MNRAS* 367, 103 (2006)
- [159] M. Dotti, M. Colpi, F. Haardt, and L. Mayer, *MNRAS* 379, 956 (2007)
- [160] M. Dotti, M. Ruzskowski, L. Paredi, M. Colpi, M. Volonteri, and F. Haardt, to appear in *MNRAS* (arXiv:0902.1525)
- [161] F. C. van den Bosch, G. F. Lewis, G. Lake, and J. Stadel, *ApJ* 515, 50 (1999)
- [162] S. E. Arena and G. Bertin, *A&A* 463, 921 (2007)
- [163] F. J. Sanchez-Salcedo and A. Brandenburg, *MNRAS* 322, 67 (2001)
- [164] N. I. Shakura and R.A. Sunyaev, *A&A* 24, 337 (1973)
- [165] C. F. Gammie, *ApJ* 553, 174 (2001)
- [166] J. Goodman, *MNRAS* 339, 937 (2003)
- [167] G. Lodato and W. K. M. Rice, *MNRAS* 351, L630 (2004)



- [168] G. Lodato and W. K. M. Rice, MNRAS 358, L1489 (2005)
- [169] G. Lodato, Nuovo Cimento 30, 293 (2007)
- [170] D. N. C. Lin and J. Papaloizou, MNRAS 186, L799 (1979)
- [171] D. N. C. Lin and J. Papaloizou, MNRAS 188, L191 (1979)
- [172] P. Artymowicz and S. H. Lubow, ApJ 421, 651 (1994)
- [173] D. Syer and J. C. Clarke, MNRAS, 277, 758 (1995)
- [174] A. Gould and H. W. Rix, ApJ 532, 29 (2000)
- [175] V. Springel, MNRAS 364, 1105 (2005)
- [176] J. Cuadra, P. J. Armitage, R. D. Alexander, and M. C. Begelman, MNRAS 393, 1423 (2009)
- [177] K. Hayasaki, S. Mineshige, Shin, and L. C. Ho, ApJ 682, 1134 (2008)
- [178] K. Hayasaki K., PASJ, in press (arXiv:0805.3408) (2009)
- [179] K. Hayasaki and A. T. Okazaki, ApJ 691, L5 (2009)
- [180] P. B. Ivanov, J. C. B. Papaloizou, and A. G. Polnarev, MNRAS, 307, 79 (1999)
- [181] A. I. MacFadyen and M. Milosavljevic, ApJ 672, 83 (2008)
- [182] P. J. Armitage and P. Natarajan, ApJ 634, 921 (2005)
- [183] B. F. Schutz, *Nature* 323, 310 (1986)
- [184] B. Kocsis and A. Loeb, Phys. Rev. Lett. 101, 1101 (2008)
- [185] P. J. Armitage and P. Natarajan, ApJ 567, L9 (2002)
- [186] M. Milosavljevic and E. S. Phinney, ApJ 622, L93 (2005)
- [187] M. Dotti, R. Salvaterra, A. Sesana, M. Colpi, and F. Haardt, MNRAS 372, 869 (2006)
- [188] Z. Lippai, Z. Frei, and Z. Haiman, ApJ 676, L5 (2008)
- [189] J. D. Schnittman and J. H. Krolik, ApJ 684, 835 (2008)
- [190] R. M. O’Leary and A. Loeb, MNRAS 383, 86 (2008)
- [191] S. Komossa and D. Merritt, ApJ 683, L21 (2008)
- [192] D. Merritt, J. D. Schnittman and S. Komossa, ApJ in press (arXiv:0809.5046) (2009)
- [193] B. Devecchi, E. Rasia, M. Dotti, M. Volonteri and M. Colpi, M., MNRAS 394, 633 (2009)
- [194] I. Berentzen, M. Preto, P. Berczik, D. Merritt, and R. Spurzem, ApJ 695, 455 (2009)